2015-11-01

The effect of interbedding on shale reservoir properties

Raji, M

10.1016/j.marpetgeo.2015.04.015
Marine and Petroleum Geology

Marine and Petroleum Geology 67 (2015) 154–169

Contents lists available at ScienceDirect

Marine and Petroleum Geology

journal homepage: www.elsevier.com/locate/marpetgeo

Research paper

The effect of interbedding on shale reservoir properties

Munira Raji [a], Darren R. Gröcke [a, *], H. Chris Greenwell [a], Jon G. Gluyas [a], Chris Cornford [b]

[a] Department of Earth Sciences, Durham University, South Road, Durham, DH1 3LE, United Kingdom
[b] Integrated Geochemical Interpretation Limited (IGI Ltd), Hallsannery, Bideford, Devon, EX39 5HE, United Kingdom

ARTICLE INFO

Article history:
Received 12 December 2014
Received in revised form
7 April 2015
Accepted 20 April 2015
Available online 29 April 2015

Keywords:
North Sea
Unconventional petroleum
Kimmeridge Clay Formation
Oil shale
Hot shale
Rock Eval
Oil Saturation Index

ABSTRACT

North Sea oil is overwhelmingly generated in shales of the Upper Jurassic – basal Cretaceous Kimmeridge Clay Formation. Once generated, the oil is expelled and ultimately migrates to accumulate in sandstone or carbonate reservoirs. The source rock shales, however, still contain the portion of the oil that was not expelled. As a consequence such shales and juxtaposed non-source lithofacies can form the targets for the exploration of 'unconventional oil'.

In this paper, we examine part of the Kimmeridge Clay Formation as a hybrid shale resource system within which 'Hot Shale' and organic-lean sandstone and siltstone intervals are intimately interbedded. This hybrid system can contain a greater volume of oil because of the increased storage capacity due to larger matrix porosities of the sand-silt interbeds, together with a lower adsorptive affinity in the interbedded sandstone. The relationship between the estimated volume percentages of sand and mudstone and free oil determined from Rock-Eval® S1 yields is used to place limits on the drainage of oil from source mudstone to reservoir sand at the decimeter scale. These data are used to determine oil saturations in interbedded sand-mudstone sequences at peak oil maturity. Higher values of free hydrocarbon (as evidenced by the S1 value in mudstone) suggest that more oil is being retained in the mudstone, while higher S1 values in the interbedded sands suggest the oil is being drained to saturate the larger pore spaces. High silica content in the interbeds confirms the brittleness in this mudstone –sandstone lithofacies – an important factor to be considered for fracture stimulation to successfully work in a hybrid system. The key points of this hybrid unconventional system are the thickness, storage capacity and the possibility to capture a portion of the expelled, as well as retained oil.

1. Introduction

The Upper Jurassic–basal Cretaceous Kimmeridge Clay Formation of the North Sea is an active generating source rock for conventional oil and gas (Barnard and Cooper, 1981; Barnard et al., 1981; Goff, 1983; Cooper and Barnard, 1984; Cornford, 1984, 1998), with further potential as an unconventional hydrocarbon reservoir. It may be something of a paradox that the Kimmeridge Clay Formation is neither Kimmeridgian (it is mainly Volgian–Ryazanian in age) nor is it a claystone, with silt-sized particles dominating as demonstrated below. A recent re-evaluation of the extensive Kimmeridge Clay Formation source rock and interbedded silicate-rich intervals have located potential for unconventional resource sweet-spots in terms of thickness, organic-richness, oil quality, maturity together with appropriate lithology, mineral content and natural fractures in the South Viking area of the North Sea (Cornford et al., 2014).

The present study focuses on 4 selected wells in UK Quadrant 16 in the southern part of the South Viking Graben of the North Sea (Fig. 1). The South Viking Graben is located within the United Kingdom (UK) and Norwegian sectors of the northern North Sea, and is bounded by the East Shetland Platform to the west and the Utsira High to the east. The 4 sampled wells lie in the UK sector of the Southern Viking Graben, with 3 of the wells (16/17-14, 16/17-18 and 16/17-19) drilled in the area where the Upper 'Hot Shale' Member is underlain by the fault-related clastic fans of the Brae Member of the Kimmeridge Clay Formation (Fig. 2). The fourth well (16/18-2) was drilled in a more axial position where the Hot Shales are underlain by more distal facies of the Brae Member fans.

The formation of the Viking Graben was initiated during the Permo-Triassic from different phases of extension followed by regional subsidence (Glennie, 1986; Erratt et al., 2010). During the Middle Jurassic a domal uplift in the central area of the North Sea

* Corresponding author.
E-mail addresses: munira.raji@durham.ac.uk (M. Raji), d.r.grocke@durham.ac.uk (D.R. Gröcke), chris.greenwell@durham.ac.uk (H.C. Greenwell), j.g.gluyas@durham.ac.uk (J.G. Gluyas), chris@igiltd.com (C. Cornford).

http://dx.doi.org/10.1016/j.marpetgeo.2015.04.015

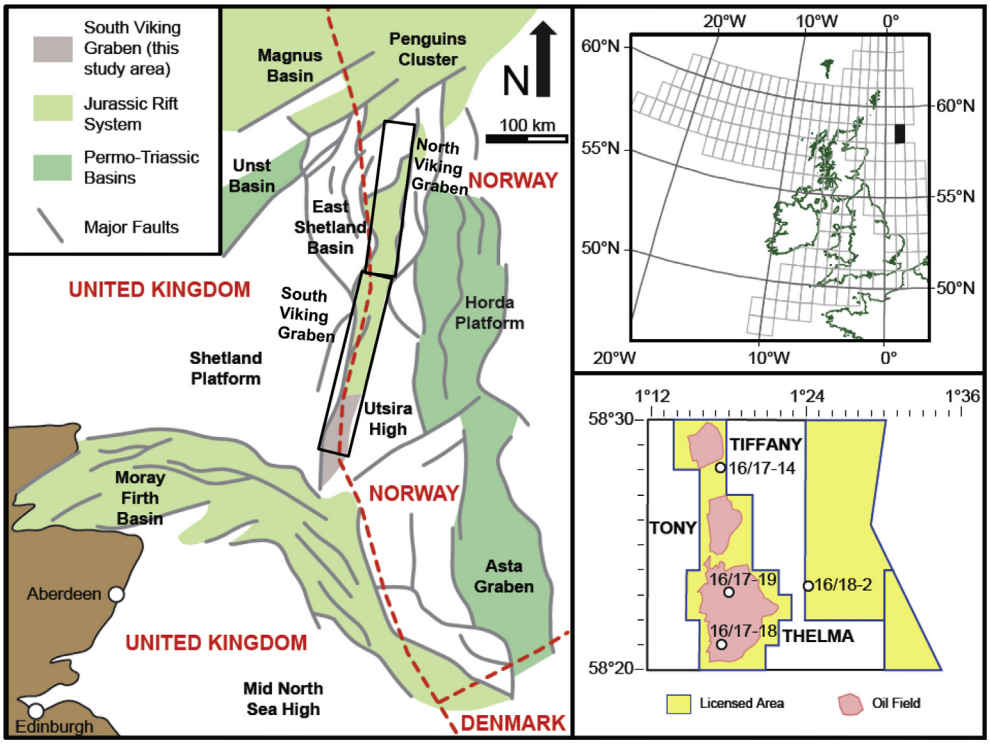

Figure 1. Structural elements of the North Sea showing the framework of the Viking Graben (modified from Dominguez, 2007) with inset of UK Quadrant 16 showing the location of wells studied (modified from DECC, 2013).

Basins arguably initiated the development of the Central and Viking grabens. In the Late Jurassic–Early Cretaceous, block faulting and tilting created the grabens, together with some strike-slip movements offsetting the graben margin faults. These offset zones played a key role in focussing coarse clastics into the deep water of the grabens, which forms the submarine fans of the Brae Member in UK Quadrant 16 (Stow, 1983; Turner et al., 1987).

Separation of the Viking Graben into northern and southern sectors occurred during structural development in the Jurassic (Richards et al., 1993). In the Middle Jurassic (Callovian–Oxfordian), structural extension produced continuous rapid subsidence in these grabens. These processes combined to produce a relatively isolated deep water basin which became relatively sediment-starved in the Upper Jurassic. With a distal connection to the Boreal seaway far to the north and in the absence of water circulation, the deep restricted basins accumulated marine Kimmeridge Clay sediments rich in organic matter (Cornford and Brookes, 1989; Gautier, 2005).

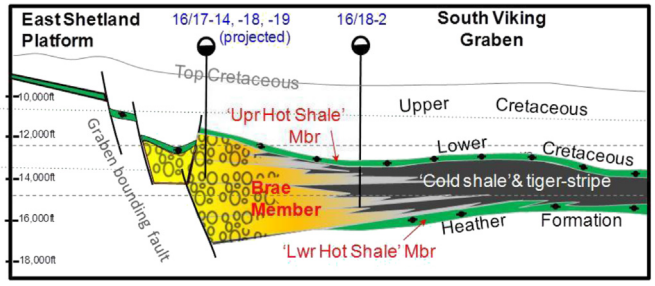

Figure 2. Schematic cross section of the Southern Viking Graben showing the facies relationship between the Upper and Lower Hot Shale and Brae members of the Kimmeridge Clay Formation.

Rapid subsidence and burial favours the maturation of the accumulated source rocks with oil generation beginning in the Cretaceous with peak generation during the Tertiary. During the Upper Jurassic to Early Cretaceous (Kimmeridgian to Ryazanian), the active western graben margin fault shed coarse clastics to form Brae Formation conglomerates and sands into the deep water trough of the south Viking Graben (Partington et al., 1993). The pebbly to fine sandstones of the Brae Formation are interpreted as proximal deep-water slope apron fans derived from the East Shetland Platform and Fladen Ground Spur (Underhill, 1998; Justwan et al., 2005; Stow, 1983). The organic-rich mudstone and interbedded fan sands, together with distal and inter-fan areas, form the basis of a sweet spot for a hybrid unconventional petroleum system (Fig. 2).

Though deep water persisted, bottom water oxygenation returned in the Early Cretaceous as the graben became a connection between the Boreal and Tethys oceans (Cornford and Brookes, 1989). By the Late Cretaceous, rifting in the North Sea region essentially ceased, with regional thermal subsidence most prominent near the axis of the abandoned rift resulting in basin depocenters for syn- and post-rift sediments (Cornford and Brookes, 1989; Ziegler, 1990; Cooper et al., 1995; Faerseth, 1996; Gautier, 2005; Johnson et al., 2005; Erratt et al., 2010).

The Kimmeridge Clay Formation is a mature source rock for both oil and gas in the graben centre. This interpretation is based on measured maturity parameters such as vitrinite reflectance and Rock-Eval T_{max} (Cornford et al., 2014), thermal modelling (Schlakker et al., 2012), direct measurement of oil generation within the source rock from solvent extraction and Rock-Eval S1 yields (Schaefer et al., 1990) and oil/source rock correlations based on molecular maturity parameters (Cornford et al., 1983). Burial history modelling, calibrated against measured parameters, suggest a burial depth deeper than 3200 m below sea bed for maturity and generation from the typical Type II oil-prone kerogen (Cornford, 1998).

As well as oil generation, deep burial of the mudstones leads to loss of porosity (mainly by compaction) and permeability (assisted by diagenetic cementation). Inter-granular pore systems within interbedded sandstone from Miller and Kingfisher Fields in UK Quadrant 16 average up to about 10 vol. % (Gluyas et al., 2000; Marchand et al., 2002; Spence and Kreutz, 2003). The porosity of the mudstones is less well constrained, however, Cornford et al. (2014) reported bulk volumes in the range of 5%.

Unconventional oil and gas is defined as oil and gas exploitable by directly drilling and fracturing of low permeability fine grained rocks acting as both source and reservoir (Jarvie et al., 2007; Abrams et al., 2014). For both unconventional oil and unconventional gas, the fine-grained rocks should be sufficiently thick and contain mid to late mature organic matter. Decomposition of organic-rich kerogen (and probably the related bitumen) yields liquid and gas, as well as potential for organic-hosted porosity as shown by numerous Scanning Electron Microscope (SEM) images (Loucks et al., 2009; Bernard et al., 2013). Reservoir properties for unconventional resource assessment include; lithology, thickness, organic matter-richness, kerogen types, thermal maturation, burial/uplift history, timing, mineralogy, fracture networks, fluid properties (density, viscosity, water saturation, phase behaviour) and expulsion efficiency (Jarvie et al., 2007, 2013; Abrams et al., 2014). Optimum combinations of these properties can be used to predict and identify sweet spots, though the controlling processes seem to vary from basin to basin. There is limited compensation within these properties, for example, a lack of maturity cannot be compensated by a greater thickness. However, whether oil or gas is produced from unconventional resources is largely a function of the source rock maturity rather than kerogen type (Jarvie et al., 2007).

Shale oil resources are defined as a source rock (organic-rich mudstones with juxtaposed organic-lean sandstone, silt) that has generated, expelled and retained oil at mostly lower thermal maturity: hence, lower temperature and pressure conditions than shale gas. The retained oil is either stored in the mudstone itself or is expelled into interbedded thin non-source facies. The term "*hybrid system*" is used to describe this type of organic-rich mudstone with juxtaposed (interbedded, underlying and/or overlying) organic-lean non-source lithofacies (Jarvie, 2012; Cornford et al., 2014). The organic-lean non-source lithofacies has less affinity for oil so it produces more readily leading to higher recovery of the original oil in place (OOIP). In contrast, organic-rich mudstone tends to retain more oil due to sorptive affinity and lower permeability (Jarvie, 2012).

At this early stage of the exploitation cycle, there are no reliable indicators for identifying commercial shale oil productivity in the UK, with the potential and resource estimates being largely based on the criteria obtained from shale oil production in the North America. Examples of hybrid systems in North America, both organic-rich, low permeability intervals and interbedded, organic-lean intervals are presently being explored in Late Devonian–early Carboniferous Bakken Formation, the Late Cretaceous Niobrara Formation (Jarvie et al., 2007; Jarvie, 2012), and arguably the Triassic Montney Formation of British Columbia (Chalmers et al., 2012; Chalmers and Bustin, 2012).

1.1. North Sea Kimmeridge Clay Formation

The Upper Jurassic Kimmeridge Clay Formation is the main source rock for the North Sea oil and gas fields in the Central and Viking Grabens. The dark, olive-grey calcareous to non-calcareous organic-rich mudstones in the Viking Graben area range in age from Volgian to Ryazanian. These sediments were deposited in a restricted marine embayment of the Boreal seaway in the north, resulting from crustal stretching and formation of the three main North Sea grabens (Cornford and Brookes, 1989; Cooper et al., 1995; Erratt et al., 2010). Sediment accumulation followed the widespread subsidence that occurred during the Late Jurassic to Early Cretaceous rifting episodes. Concomitant global sea-level rise led to the Late Jurassic marine transgression event, resulting in the Oxfordian Heather Formation, comprising of organic-lean mudstones deposited under oxic bottom water conditions. With the closing of the Boral-Tethyan connection, high sedimentation rates, elevated organic matter productivity (probably controlled by nutrient supply) and increased water depths all promoted stratified anoxic bottom waters. With greatly improved organic matter preservation, this resulted in the deposition of the thick, organic-rich Kimmeridge Clay Formation (Cornford and Brookes, 1989; Tyson, 2004).

During the Upper Jurassic, conglomerates and sands were periodically transported as submarine fans by gravity flow across the uplifted graben edge of the Shetland Platform and in to the main graben (Partington et al., 1993). These sands were fed into the basin via graben-edge 'notches' formed over ramps/transfer zones (transform fault lineations) which breached the uplifted footwall. These coarse clastics sediments, called the Brae Formation were deposited into the anoxic basin of the main South Viking Graben, where they are found interbedded with the mudstones of the Kimmeridge Clay Formation (Leythaeuser et al., 1984, 1987; Turner et al., 1987). This sediment association (Fig. 2) forms the target for the present study.

The Kimmeridge Clay Formation can be assessed as a potential shale oil reservoir since it contains actively generating source rocks and significant quantities of residual oil in the fully mature areas of the North Sea (Cornford et al., 2014). A maximum thickness of 1,100 m is recorded for the Kimmeridge Clay Formation in the South Viking Graben (Gautier, 2005), with the maturity and lithofacies of these source rocks varying laterally and vertically across the study area (Fig. 3). This illustration emphasises the need to overlap aspects of thermal maturity (upper) and of organo-facies (lower) to identify optimal 'sweet spots' for drilling unconventional wells. The interaction of facies and maturity are optimized where total organic content (TOC) values are high and the kerogen type is oil-prone. Where oil saturation is high, asphaltene contents are extremely low and resins are reduced, and the interval lies in the volatile oil window where API gravities are generally >40°API and gas/oil ratios (GORs) are in the range of 1000–15,000 scf/stb (standard cubic feet of gas/barrel of oil) (Jarvie, 2012).

In the South Viking Graben, the formation generally thickens towards the basin margin fault and thins over the crest of the intra-basinal fault blocks (Richards et al., 1993). The thickening into faults is less prominent for the Upper and Lower Hot Shale mudstones, than for the pebbly to fine sands of the Brae Formation (Fig. 2). Three gross facies are recognized: Kimmeridge Clay Hot Shale (both Upper and Lower), an intermediate facies of interbedded sands and mudstones termed the Tiger Stripe facies, and massive sand and conglomerates of the Brae Formation (Fig. 2). The Tiger Stripe facies is mainly found below the Upper "Hot Shale" and above the main Brae Formation, and comprises an alternating mudstone and fine-grained sand interbeds. It is interpreted to have been deposited by low-density turbidity currents on the outer submarine fan, inter-fan and in the basin plain environments (Reitsema, 1983; Stow, 1983; Leythaeuser et al., 1984; Turner et al., 1987; Roberts, 1991; Rooksby, 1991). Lithological and compositional heterogeneity of the mudstone–sandstone interbeds is caused in part by variation in organic richness (TOC) and kerogen type as evidenced by the core

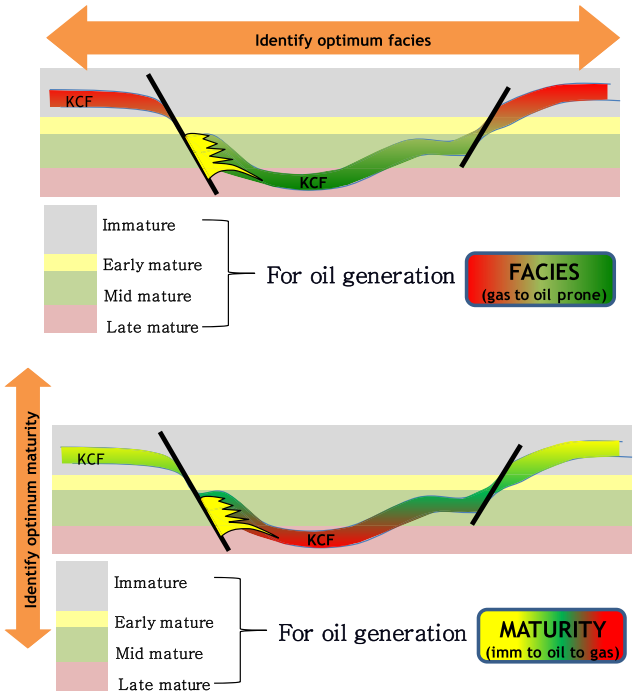

Figure 3. Identification of optimum facies (lateral), and maturity (vertical) for extracting unconventional liquids from the Kimmeridge Clay Formation of the South Viking Graben, North Sea.

samples in the study area (Huc et al., 1985; Isaksen and Ledje, 2001).

2. Methods: sampling and analytical procedures

2.1. Sampling

In this paper, eighteen core plugs from four south Viking Graben wells (16/17-14, 16/17-18, 16/17-19, 16/18-2) drilled between 1984 and 1991 were sampled from the British Geological Survey core storage in Keyworth, Nottingham UK (Fig. 4, right). The samples were selected based on the visual inspection of slabbed cores and estimates of percentage of mudstone and sandstones at different intervals from each well (Fig. 4, right). The first three wells lie on the western margin of the graben along the Tiffany-Toni-Thelma field trend, and the latter (16/18-2) is in the trough axis to the east near the UK-Norwegian boundary (Figs. 1 and 2).

In terms of depth (metres sub-Kelly Bushing), the cores from the 16/17-19 well are the shallowest (3552-82 m) followed by those from 16/17-18 at 3720-83 m. The cores from the other two wells are substantially deeper with the 16/18-2 having a short cored interval of 4126.5–28.7 m and 16/17-14 at 4193.7-4211.9 m (Table 1, appendix). Since they represent the upper part of the sequence (Upper Hot Shale and Tiger Stripe), the units sampled are taken to be Volgian to Ryazanian in age, and consists of mudstone sequences with interbedded sandstone (Fig. 2). The percentage of the mudstone and sandstone were visually estimated from full cores and core plugs initially, with the estimates being substantiated by observing thin sections under an optical microscope.

The composition of the sandstone–mudstone mineralogy and porosity distribution were derived from petrographic thin sections, X-ray diffraction (XRD) and visual core descriptions. Geochemical analyses were carried out to determine the source rock potential, kerogen-type, maturity, carbon-isotope composition and retained hydrocarbon yield.

2.2. Petrography

Eighteen petrographic thin-sections were analysed for mineralogy, rock fabric, texture, fractures and fossil contents. Thin sections were polished to approximately 20 μm in thickness. In terms of simple lithofacies, the abundance of sand in the mudstone was estimated from the thin sections, with each sample being placed in one of five categories (Fig. 4, right).

2.3. X-ray diffraction (XRD)

A Bruker D8 Advanced diffractometer set to Bragg-Brentano geometry reflection mode analysis was used to record the X-ray diffraction pattern of 17 powdered samples. The samples were prepared and mounted on a dry slide glass and held in a sample holder. The X-ray radiation was Cu K_α (1.54056 nm) and the sample was scanned between 5 and 65° 2θ angle with a 0.02° 2θ step size (Moore and Reynolds, 1997).

2.4. Total organic carbon and pyrolysis analysis

Thermal vaporization and pyrolysis analysis of powdered samples was carried out using a Rock-Eval 6 Instrument to obtain information on hydrocarbon generation, potential, type and maturity of organic matter in the samples. Norwegian Petroleum Directorate (NPD) rock standard, and Jet-Rock 1 (JR-1) standards were analysed every tenth sample and checked against the acceptable range given in NIGOGA standard documentation (Espitalié et al., 1985a; Peters, 1986; Lafargue et al., 1998; Weiss et al., 2000). The TOC (total organic carbon) content of the samples was measured on a Leco SC-632 instrument as weight percent of the initial rock sample. Prior to TOC analysis samples were treated with dilute hydrochloric acid to remove any carbonate.

2.5. Sample preparation for stable isotope analysis

Each sample was ground into fine powder using a Retsch RM100 mill. The powdered samples were placed in 50 ml centrifuge tubes, and 40 ml of 3 M HCl were poured onto the samples for decalcification and left to stand overnight. Only four samples (from 3572.0 m in well 16/17-19, and 3782.9 m in well 16/17-18 and from 4211.7 m to 4193.6 m in well 16/17-14) showed visible moderate to violent reaction to HCl, indicating high carbonate content. All the samples were rinsed five times with deionised water to remove any residual HCl. The samples were then dried for 24 h at 50–60 °C, and then ground again using an agate mortar and pestle. Each sample was then accurately weighed into tin capsules for stable isotope analysis.

Stable isotope measurements were performed at Durham University using a Costech Elemental Analyser (ECS 4010) coupled to a ThermoFinnigan Delta V Advantage. Carbon-isotope ratios are corrected for ^{17}O contribution and reported in standard delta (δ) notation in per mil (‰) relative to the Vienna Pee Dee Belemnite (VPDB) scale. Data accuracy is monitored through routine analysis of in-house standards, which are stringently calibrated against international standards (e.g., USGS 40, USGS 24 and IAEA 600). Analytical uncertainty for $\delta^{13}C_{org}$ measurements is typically ±0.1‰ for replicate analyses of the international standards and typically <0.2‰ on replicate sample analysis. In addition to the Leco analysis mentioned above, total organic carbon was obtained as part of the isotopic analysis using an internal standard (i.e., glutamic acid, 40.82% C).

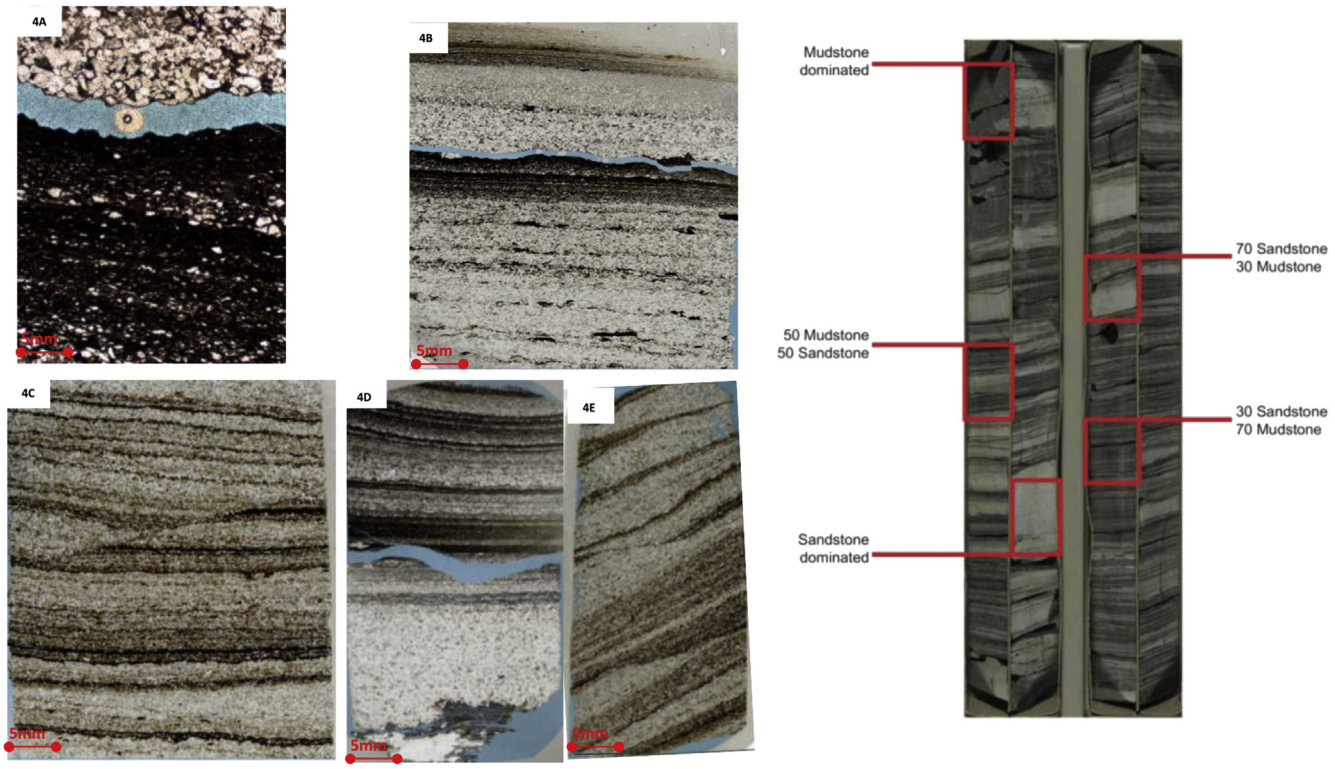

Figure 4. Left: Thin-section photomicrographs of sand-dominated mudstone interbeds: (4A) Sandstone-dominated photomicrograph thin section images from 4127.4 m (well 17/18-2); (4B) Sandstone alternating with organic-rich mudstone layers, impregnated with blue-dyed resin showing breakage at the contact boundary between sandy and muddy layer (probably core disintegration during drilling and sampling); (4C) Organic-rich 70/30 sandstone/mudstone from 3552 m (well 16/17-19); (4D) 50/50 sandstone/mudstone with desiccation fractures from 4126.2 m (well, 16/18-2); (4E) organic-rich sandstone–mudstone from 3, 582.9 m (well 16/17-19). Right: Example core photograph showing regions that were sampled based on a visual estimate of the percentage of sand and mud.

3. Results and discussions

3.1. Mudstone and sandstone mineralogy

Observations from 18 thin-sections suggest that, generally, the interbedded sandstones are fine-medium grained sands, with silty high organic carbon contents in the mixed sandstone/mudstones and lower organic carbon content in the purer sandstone facies (Fig. 4A–E)

The mudstone-dominated lithologies are black to dark grey, silty, partly laminated with gradational boundaries between the mudstones and the interbedded light-grey sandstones (Fig. 5A, B

Table 1
TOC and Rock-Eval Pyrolysis data for 18 core plug samples from the Kimmeridge Clay Formation of the South Viking Graben, North Sea, UK.

Well	Depth	S1	S2	S3	T_{max}	PP	PI	HI	OI	TOC	Sandstone
	(m)	(mg/g)			(°C)	(mg/g)	(S1/S1+S2))	(mg/g TOC)		(wt%)	(%)[a]
16/17-14	4200	3.61	7.11	0.20	437	11.0	0.34	132	4	5.37	30
16/17-14	4211.7	1.86	5.69	0.10	439	7.6	0.25	245	4	2.32	50[c]
16/17-14	4193.6	2.70	3.74	0.18	427	6.4	0.42	340	16	1.10	90[c]
16/17-14	4194.7	5.42	11.10	0.25	437	17.0	0.33	152	3	7.32	10
	Average	*3.4*	*6.91*	*0.18*	*435*	*10.5*	*0.34*	*217*	*6.8*	*4.02*	
16/17-18	3719.8	5.51	12.30	1.06	428	18.0	0.31	221	19	5.54	10
16/17-18	3780.4	2.50	3.09	0.15	431	5.6	0.45	151	7	2.04	50
16/17-18	3781.4	4.53	10.9	0.34	435	15.0	0.29	167	5	6.51	30
16/17-18	3782.9	1.20	2.32	0.24	431	3.5	0.34	329	34	0.71	90[c]
	Average	*3.43*	*7.15*	*0.45*	*431*	*10.5*	*0.34*	*217*	*16.3*	*3.70*	
16/17-19	3552.2	1.68	2.34	0.16	427	4.0	0.42	257	18	0.91	70
16/17-19	3564.1	3.99	15.30	0.40	430	19.0	0.21	291	8	5.25	30
16/17-19	3572.0	4.27	21.40	0.10	430	26.0	0.17	354	2	6.06	10[c]
16/17-19	3574.8	2.72	6.34	0.16	433	9.1	0.30	334	8	1.90	90
16/17-19	3582.7	3.42	4.64	0.47	432	8.1	0.42	243	25	1.91	50
	Average	*3.20*	*10.00*	*0.26*	*430*	*13.2*	*0.30*	*296*	*12.2*	*3.20*	
16/18-2	4126.0	3.19	33.10	0.48	436	36.0	0.09	368	5	8.99	10
16/18-2	4126.2	1.54	22.50	0.20	434	24.0	0.06	352	3	6.38	50
16/18-2	4127.7	1.87	14.60	0.49	432	17.0	0.11	311	10	4.70	70
16/18-2	4127.4	1.32	4.92	0.12	434	6.2	0.21	286	7	1.72	90
16/18-2	4128.4	2.38	14.00	0.08	429	16	0.15	276	2	5.08	30
	Average	*2.06*	*17.82*	*0.27*	*433*	*19.8*	*0.12*	*319*	*5.4*	*5.37*	

[a] Visual estimate of area, error taken as ±5%; samples marked 'c' reacted with HCl and hence contained significant carbonate.

and D). At this magnification it is clear that even the mudstone-rich samples contain mainly silt (2–63 μm), with little to no clay-sized fraction (<2 μm) apparent.

X-ray diffraction (XRD) results suggest these samples are dominated by quartz, clay, organic matter and pyrite (Fig. 6). Kaolinite, illite/smectite and some chlorite are the dominant clay minerals identified in all samples. In general, a more intense XRD peak for quartz is observed in the sandstone dominated samples, though fine quartz is also a significant fraction of the mudstones. Brittleness measures the amount of stored energy within the grains prior to failure, which is controlled by the temperature, effective stress from burial, diagenesis texture, total organic carbon content and fluid type. The abundance and preservation of silicate minerals (Fig. 6) in the sand-rich samples suggest little diagenetic alteration, as expected given the limited depth range, with the primary quartz content likely to exert control on the brittleness of the interbedded sandstone and mudstone.

Kaolinite, a non-swelling clay is able to absorb petroleum while illites are able to absorb pore water which increases the wettability of these samples (Arduini et al., 2009). However, smectite (a swelling clay) hinders the flow of fluid in the pore space leading to low permeability and reduced porosity (Kwon et al., 2004; Arduini et al., 2009). The ratio of illite–smectite can be used to estimate the level of maturity (%Ro) and hence oil generation during burial relating to diagenesis and catagenesis. However, smectite to illite conversion is more sensitive to time than temperature compared with changes in vitrinite reflectance (Hillier et al., 1995). Diagenetic alteration of clay minerals during burial in the South Viking Graben (well 16/22-2) is reported by Pearson et al. (1983), and shows an initial increase of 70–100 % smectite (Oligocene–Eocene; 1500–2500 m), followed by an abrupt increase back to 70% in the Paleocene (2500–2800 m) and then little change to 3500 m (Paleocene – Campanian). Below this depth a decrease to 20% smectite is observed from the Campanian through

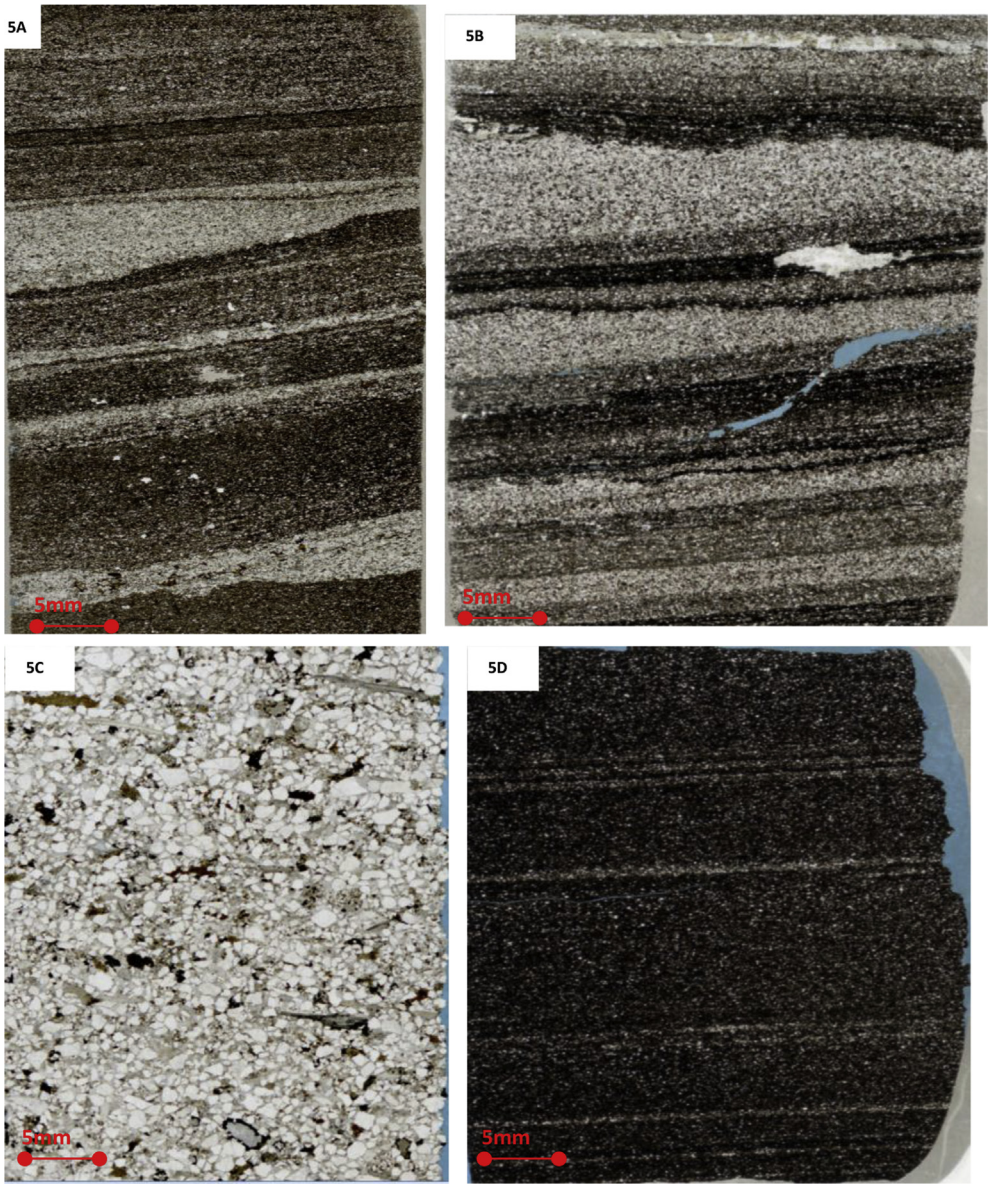

Figure 5. Thin-section photomicrographs of hybrid shale system displaying various mudstone–sandstone interbeds: (5A) 30/70 sandstone/mudstone fine-medium sandstone, dark-grey, sub-angular-sub-rounded, moderately sorted from 3564.1 m (well 16/17-19); (5B) 50/50 sandstone/mudstone with darker organic-rich layers from 3780.4 m (well 16/17-18); (5C) Sandstone dominated sample with visible shell fragments and woody (Type II kerogen) remnants from 4193.6 m (well 16/17-14); (5D) mudstone-dominated samples from 4194.7 m (well 16/17-14), the light-grey colour within the mudstone are thin siliceous sandstone layers, some only a grain thick.

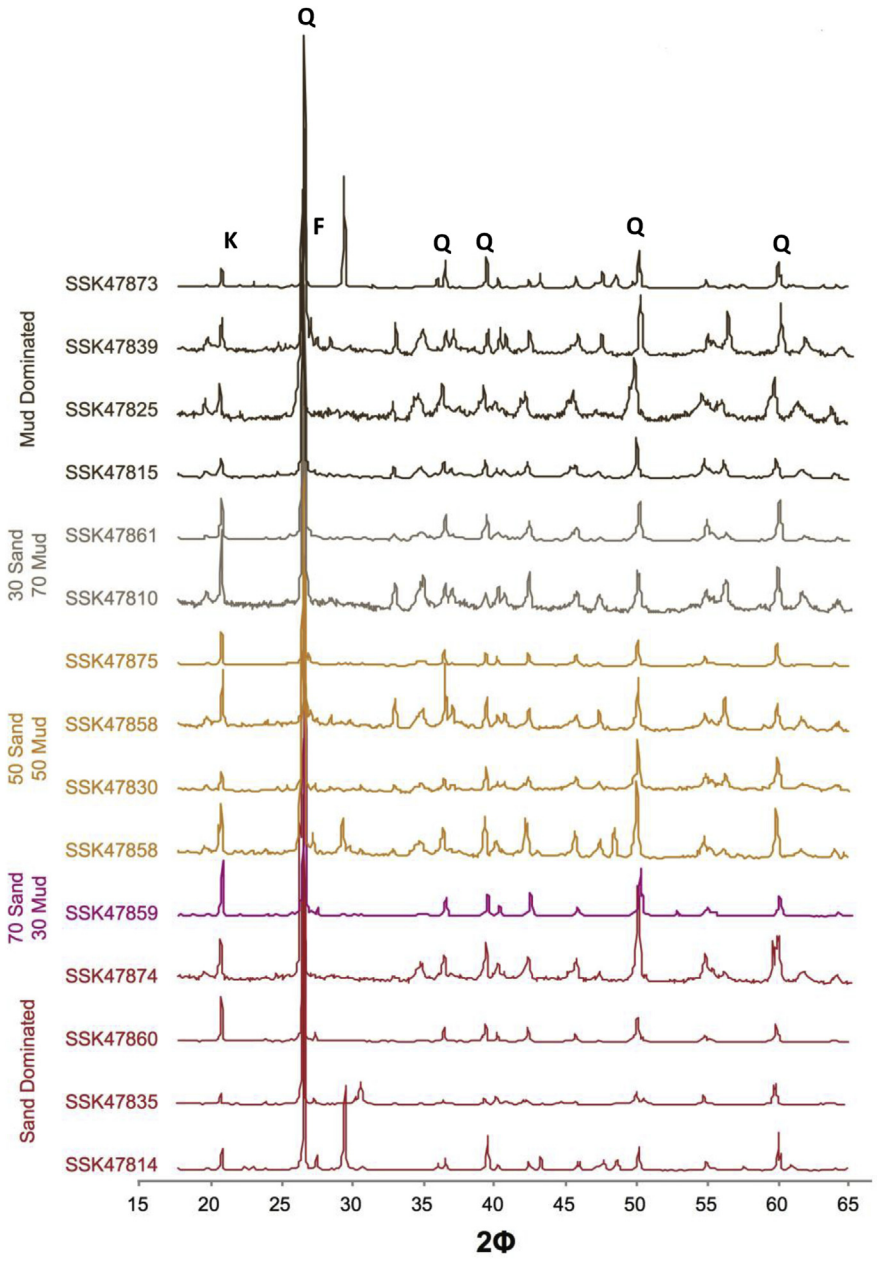

Figure 6. X-ray diffraction (XRD) pattern (Cu Kα radiation) of sandstone and mudstones samples. Q = Quartz, K = Kaolinite, F = Plagioclase Feldspar.

to the Middle Jurassic at and below 4000 m. This non-linear trend illustrates a combination of the effects of lithofacies for shallow (cool) samples, and a dominance of catagenesis at depth. Given the proximity of the well reported by Hillier et al. (1995) and the likelihood of a similar thermal profile, the presence of smectite in the samples of the present study from below 4000 m suggest control from the former rather than the latter process.

The XRD trends for the clay minerals are similar to the Kimmeridge Clay Formation type-section in Dorset, which has a much lower maturity, deposited in shallower water and is co-eval with the Lower Hot Shale (Hallam et al., 1991; Hesselbo et al., 2009; Farrimond et al., 1984). The observed mineralogy from these present samples is comparable to the recorded Nordland Shale mineralogy from UK Quadrant 16 and Norwegian Quadrant 16 (Lothe and Zweigel, 1999; Kemp et al., 2001). Finding an area in this hybrid system that is brittle may be a key factor in creating vertical fracture pattern that are large enough to connect the highest amount of rock volume during hydraulic fracturing stimulation.

3.2. Carbon isotope composition of the kerogens

Carbon isotope ratios are used to classify the origin of organic matter in terms of marine (aquatic) or continental (land) plant origins (Meyers, 1994; Galimov, 2006), with stratigraphically restricted deviations based on global climate variation (e.g., Jenkyns et al., 2002; Jarvis et al., 2011) and on changes in sea level (e.g., Gröcke et al., 2006; Jarvis et al., 2011). Carbon and nitrogen (C/N) ratios and organic $\delta^{13}C$ values may be used to place limits on the source of the organic matter in sediments (Meyers and Eadie, 1993), together with post-depositional changes of the original organic input (Calvert, 2004). The $\delta^{13}C_{org}$ values for the investigated samples range from −29.7‰ to −26.9‰, which are typical of marine organic

matter (Meyer et al., 1984a; Meyer and Benson, 1988) or *n*-alkanes derived from land plant leaf waxes (Meyers, 1994).

For the Quadrant 16 samples, both sandstones and mudstones have a common projected origin of 30‰ for the plot of TOC vs kerogen stable carbon isotope values (Fig. 7). Different gradients are noted for mudstone-dominated and sandstone-dominated samples from the 4 wells. The sandstone gradient of 1.3‰ units/1 % TOC suggests the increase in TOC derives from the addition of isotopically heavy macerals, such as vitrinite. This is consistent with the particulate kerogen seen in the sand-dominated thin section shown in Figure 5c. This suggests that isotopically heavy land plant fragments from the Shetland Platform, presumably carried by the rivers transporting the fan sands, are the main contributors to the TOC in the sandstones.

In contrast the mudstones form a cluster of eight high TOC samples (mean TOC = 6.4%), and have carbon isotope values with a mean of $\delta^{13}C = -28.2‰$). At 0.3‰ units per 1% TOC, the mudstone gradient in Figure 7 is much lower than the sandstones suggesting the mixing and preservation of an isotopically light end member is controlling the gross organic matter properties. Such values probably reflect bacterially degraded algal organic matter found in North Sea Kimmeridge Clay mudstones (Galimov, 2006).

This interpretation is supported by the relationship between the carbon isotopes and Hydrogen Index (HI), which is used as an indicator of kerogen type at comparable maturities (Fig. 8). The majority of the data in Figure 8 show that low HI samples (gas prone and presumably vitrinite rich) have isotopically heavier carbon, and the higher HI samples are isotopically lighter. This fits well with other data from Viking Group shales in adjacent wells (Fig. 8).

The trends for C/N against TOC show a steep increase in C/N for the mudstone rich samples, but a shallower gradient for the sand-rich samples (Fig. 9). This is to be expected in the sandstones which are dominated by terrestrial organic matter. High organic carbon content and high C/N values from the mudstone-rich samples suggest that there is enhanced preservation of algal-bacterial carbon as well as terrestrial organic matter, and/or relative depletion of nitrogen rich proteinaceous material (Jenium and Arthur, 2007).

The kerogen type in both the mudstones and sandstones is predominantly a typical Type II oil (and associated gas) prone kerogen. However, based on isotope bulk properties such as $\delta^{13}C_{org}$ and C/N ratios, separate trends against TOC are noted for sandstones and for mudstones. This can be explained by a uniform

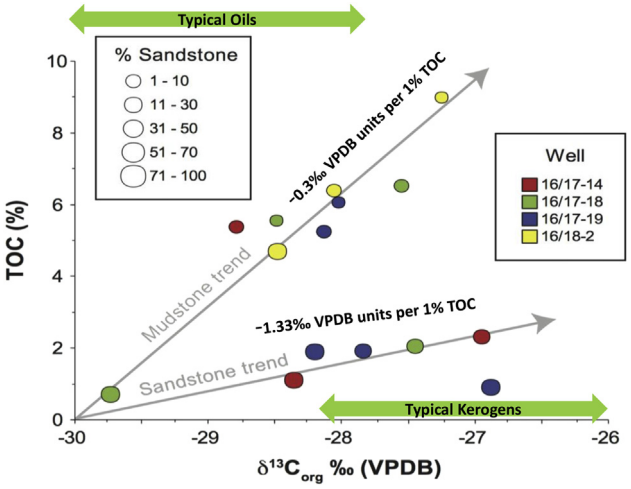

Figure 7. Relationship of TOC and $\delta^{13}C$ of organic matter between sandstone and mudstone samples for the Upper Jurassic of UK Quadrant 16.

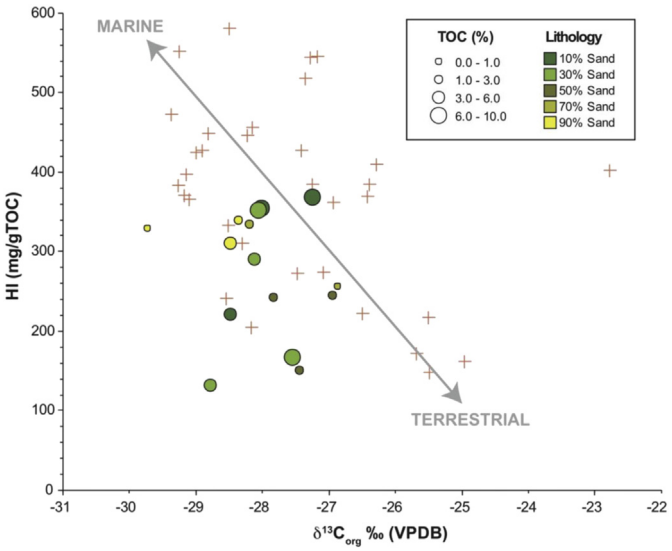

Figure 8. HI (kerogen and maturity dependent) plot *versus* carbon isotope ratios of organic matter from core depths between 3500–4300 m (UK Quadrant 16, South Viking Graben). Red crosses are from equivalent public data in adjacent Norwegian wells (NPD 2015). (For interpretation of the references to colour in this figure legend, the reader is referred to the web version of this article.)

background of bacterially degraded algal organic matter, with the isotope and nitrogen composition reflecting the residue of different bacterial metabolic pathways (sulphate-reducing *versus* methane-generating bacteria). The mudstone-dominated samples, with expected low sedimentation rates, show increasing (heavier) isotope values per 1% increase in TOC, which would be consistent with a dominance of sulphate-reducing bacterial degradation. Carbon loss will be dominated by isotopically heavier bacterial CO_2, leaving an isotopically lighter residue.

In contrast, the sandstone-dominated samples show strongly increasing (heavier) kerogen isotope values per 1% increase in TOC, suggesting degradation dominated by methanogenesis. Carbon loss will be dominated by isotopically light bacterial CH_4, leaving an isotopically heavier residue. Thus in both cases the Type II kerogen is bacterially degraded, but with different bacterial metabolisms dominating.

3.3. Richness, source and maturity of organic matter in the Kimmeridge Clay interbeds

TOC content and Rock-Eval pyrolysis values for samples in this study are reported in Table 1, and are shown plotted against depth in Figure 10. No consistent depth trends are seen with most variation, particularly for TOC and S2 values, correlating with the sandstone/mudstone abundance for each well.

In terms of overall organic richness, the samples containing a high proportion of mudstone (70% or more of mudstone) have good to very good TOC values by industrial standards (Cornford, 1998). Nine of these samples are characterized by TOC values ranging from 5.1 to 9.0 wt % (mean = 6.3 ± 1.3 wt % TOC). A plot of the % sandstone values *versus TOC* (Fig. 11) shows a steeper gradient for the sandier samples (≥50% sand) projecting to ~0.5% TOC for 100% sand. In contrast, there is more scatter and a lower gradient for the mud-dominated samples, with a poorly defined trend projecting to 8–10% TOC for a pure mudstone end member (Fig. 11).

In well 16/18-2 at 4127.7 m, a sample with a dominance of sandstone (70% sandstone) recorded a TOC value as high as 4.7 wt % (Fig. 11). This sample comes from a more basinal well, and the

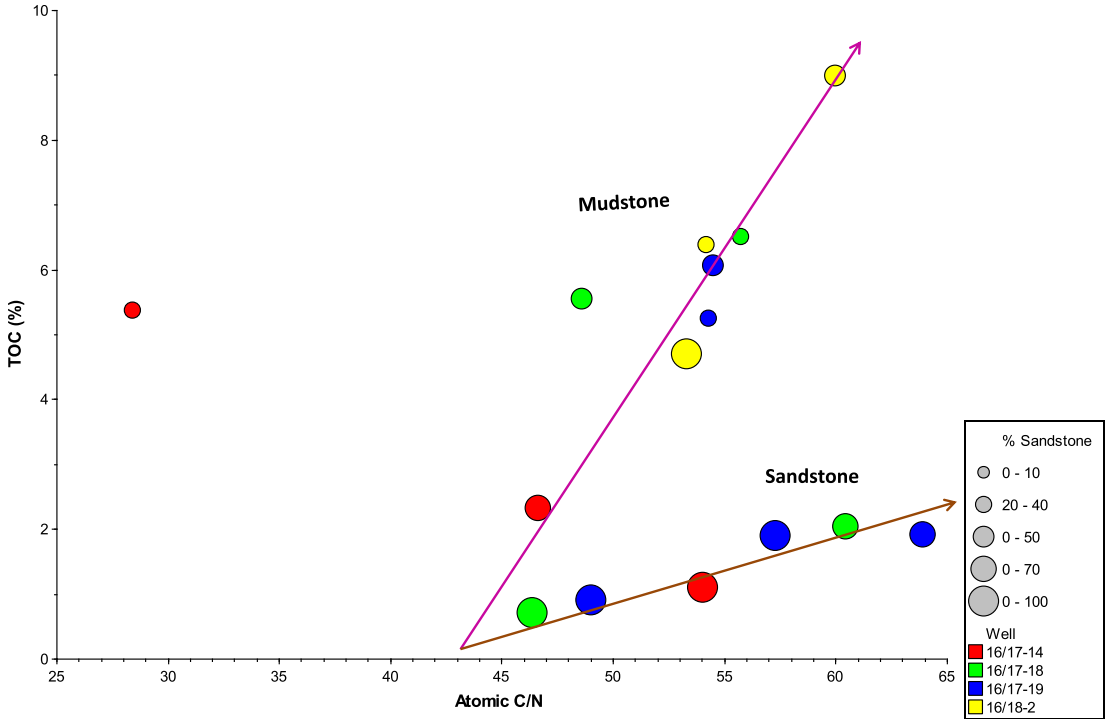

Figure 9. Relationship between TOC and C/N ratio showing different trends for sandstone-dominated and mudstone-dominated samples for core plugs from four Quadrant 16 wells, UK. Note the one anomalous point with high TOC and a low C/N atomic ratio.

Hydrogen and Oxygen indices (Table 1) suggest that the kerogen type is of the marine bacterial–algal Type II composition. This may indicate that a lots more of the interstitial space within this sandstone is rich in organic matter, which is not apparent on a visual inspection.

The measured TOC values in this study are similar to those previously reported in the North Sea. For example, Isaksen et al. (2002) recorded TOC values ranging from 3 to 10 wt % in the Upper Draupne (Kimmeridge Clay) Formation, and 2-5 wt % for organically leaner Lower Draupne and Heather Formations in Norway. Average TOC values of 5.6 wt % from 2600 to 3200 m and 4.9 wt % from 3250–3650 m were also reported from the Kimmeridge Clay Formation in the Viking Graben (Goff, 1983). Fuller (1980) also found an average of 3.3 wt % in sediments from the

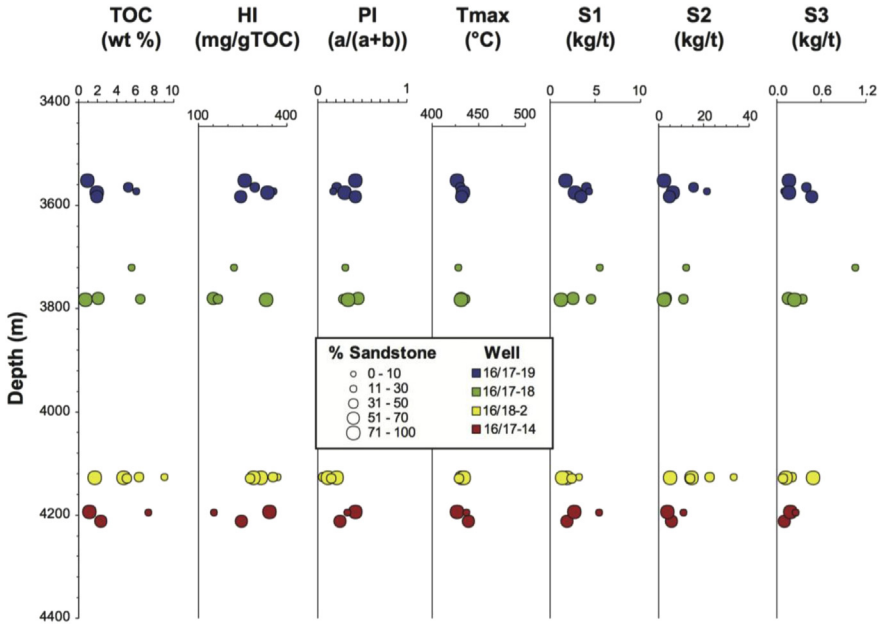

Figure 10. Relationships for TOC and Rock-Eval parameters *versus* depth for core plugs from the Kimmeridge Clay Formation intersected by four wells at different depths within Quadrant 16, South Viking Graben, UK.

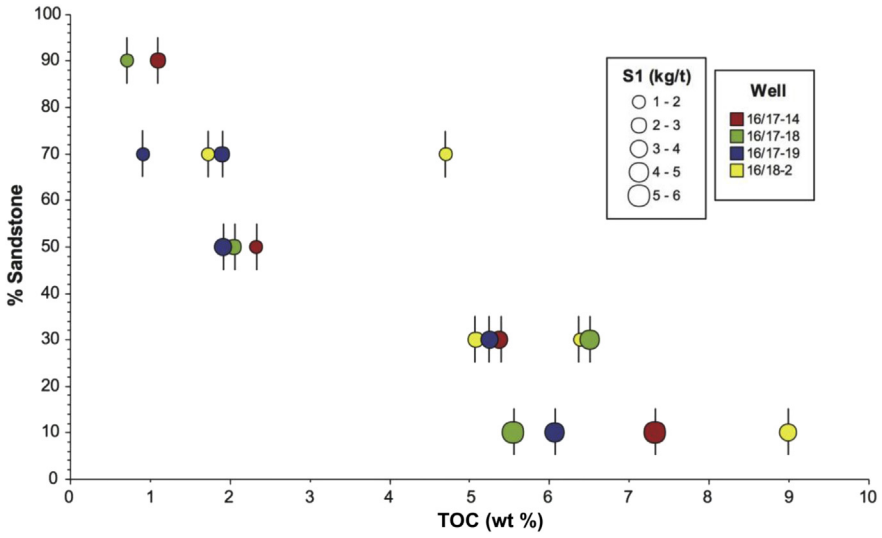

Figure 11. Total Organic Carbon (TOC wt %) as a function of sandstone abundance showing two trends and projecting an average 0.5 wt % TOC for a 100% sandstone end member and ~9wt % TOC for a 100% mudstones end member.

Kimmeridge Clay Formation in general. These values suggest that the source rocks contain high amounts of organic matter, which has been shown to be adequate for shale oil generation (Jarvie, 2012).

Origin and types of organic matter were determined mainly from Rock-Eval analysis, using plots of Hydrogen Index (HI) *versus* T_{max}, HI *versus* Oxygen Index (OI), and TOC *versus* S2 (remaining petroleum generation potential). The new UK Quadrant 16 values are plotted in the context of the public access data in the Norwegian Petroleum Directorate (NPD) of Upper Jurassic Viking Group samples from Norway Quadrant 15 (Fig. 12).

The Hydrogen Index *versus* T_{max} data from this study (Fig. 12, upper) fits with the regional maturity trend from Norway Quadrant 15 and with a typical Type II kerogen trend based on the maturity trends. Fitting with the well-defined Norwegian trend indicates that the initial kerogen was Type II containing bacterially degraded algal kerogen, with a few samples plotting towards Type I kerogens containing better preserved algae (Cornford, 1998). The relationship between HI *versus* OI, a pseudo-van Krevelen plot (Fig. 12, lower), suggests that most of the UK samples are a mix of Type I (mainly algal) and Type II (bacterially-degraded algal) kerogens, though this is based largely on low Oxygen Indices. In contrast to TOC (Fig. 11), the sand-rich and mudstone-rich samples plot together in terms of kerogen type for both graphs shown in Figure 12.

The effect of kerogen quantity being linked to the sand-mudstone ratio, while kerogen type is independent, is shown by the standard S2 *versus* TOC plot (Fig. 13). Whilst the sand rich samples plot with low S2 and TOC values, they fall on the same iso-HI line of 300 mg/g TOC as the majority of the richer samples. The extent to which the sand-rich samples fall below the HI = 300 mg/g TOC line reflects the amount of terrigenous Type III kerogen in the mix. This discrepancy in kerogen type assignment may also occur because the S2 *versus* TOC plot overlay is based on immature organic matter, and not mature samples such as those from the deep wells sampled in UK Quadrant 16 (Table 1).

3.4. Interpretation of maturation and quantification of generated oil

Rock-Eval T_{max} values were used as a thermal maturity indicator, these values range from 427 °C (late immature-early mature) to 439 °C (mid-mature) with an average of 432 °C (Table 1). The samples cover a depth interval from 3552.2 m to 4212.0 m. To make literature comparisons, the T_{max} values were converted to vitrinite reflectance (Ro), using Jarvie's equation: $R_o = (T_{max} \times 0.018) - 7.16$ (Jarvie, 2001; Peters et al., 2005). The converted T_{max}-based R_o values range from 0.53 to 0.74 % R_o with an average of 0.62 % R_o suggesting that the majority of the samples are in the early-to mid-mature oil window (Fig. 14).

The maturity is similar to the 0.62% R_o oil window recorded at an average depth of 3500 m (Justwan et al., 2006), 3400 m (Isaksen and Ledje, 2001) and 3340 m (Baird, 1986) for the South Viking Graben area (Fig. 14).

The lithological differences between the mudstones and sandstones are reflected in the Rock-Eval Production Index (PI) values (Table 1), where the PI is calculated as the ratio of S1/(S1 + S2). In general, PI tracks the transformation of kerogen into free hydrocarbons (S1 kg/tonne of rock). In addition, PI is typically higher in poorly drained source rocks and lower in well drained source rocks (Cornford, 1998). In the case of the Quadrant 16 samples, the abundance of sandy layers would be expected to define drainage. However, the relationship between PI and T_{max} suggest these bulk samples (i.e. analysing the sandstone–mudstone mix as a single sample) to be poorly-drained source rocks (Fig. 15). This implies that the sandier samples have retained rather than drained oil, and hence they may enhance the producible oil in the mudstones.

The conventional interpretation of PI as an indicator of generation and retention is shown by the interpretation lines in Figure 15. The samples cover a relatively narrow range of maturity (T_{max} = 427–439 °C), but show a wide range of PI values (0.06–0.45). Figure 15 shows that there is consistent variation by well and that the PI values are independent of sandstone content. At the same maturity level based on T_{max}, the 16/18-2 well (five samples from 13,358–13,546 ft) has consistently low PI values and the 16/17-18 well (four samples from 12,205 to 12,412 ft) has consistently higher PI values.

The relationship of PI (S1/(S1 + S2)) with sand content (Fig. 16) is further investigated to test whether the sandstone layers offer storage for the oil generated in the interbedded mudstone layers. The mean PI value for each lithology group is shown as well as the individual measurements on each sample. Where mudstone dominates (<30% sand), the average PI values are low (0.21–0.23),

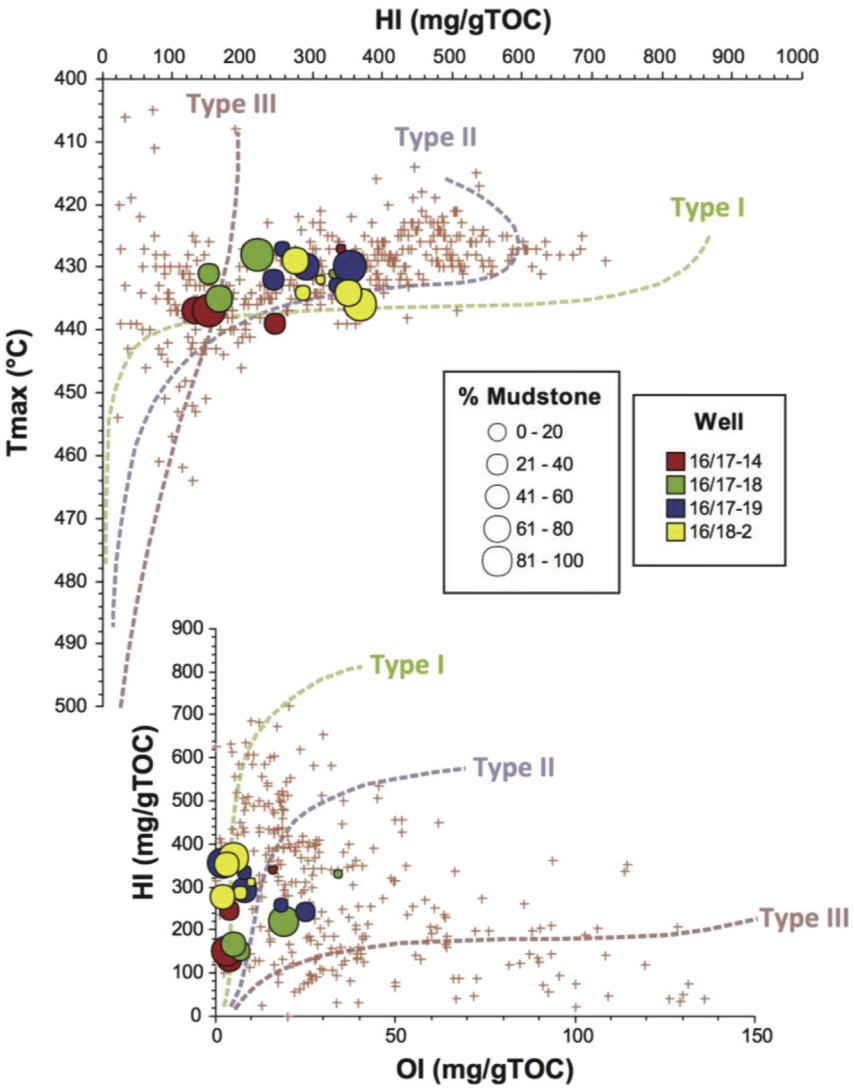

Figure 12. Kerogen type and maturity from Rock-Eval pyrolysis: the Hydrogen Index *versus* T_{max} (HIT) plot (upper) and pseudo-van Krevelen Oxygen Index (OI) and Hydrogen Index (HI) plot (lower). Red crosses represent data from the Norwegian Petroleum Directorate (NPD). (For interpretation of the references to colour in this figure legend, the reader is referred to the web version of this article.)

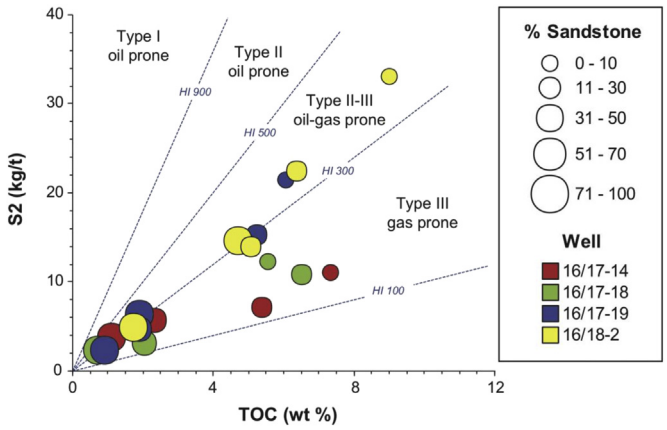

Figure 13. Relationship between Total Organic Carbon (TOC) and Rock-Eval S2 (kg pyrolysate/tonne of rock) where the diagonals are Hydrogen Index (S2/TOC, mg pyrolysate/g TOC).

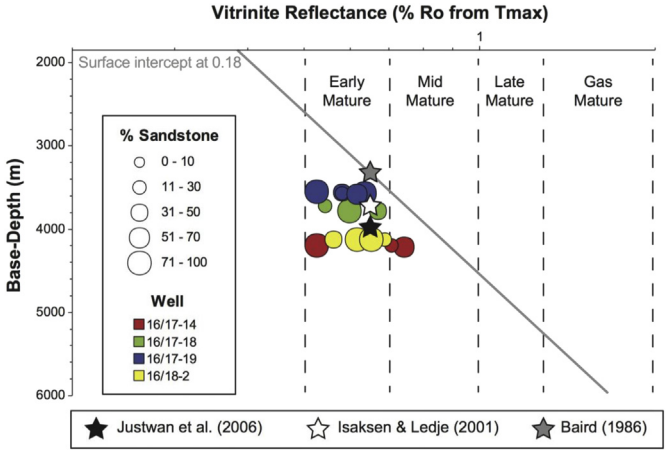

Figure 14. Thermal maturity depth plot showing early-mid mature oil generation window based on vitrinite reflectance values converted from Rock-Eval T_{max} compared with similar maturity/depth values recorded by Baird (1986), Justwan et al. (2006) and Isaksen and Ledje (2001).

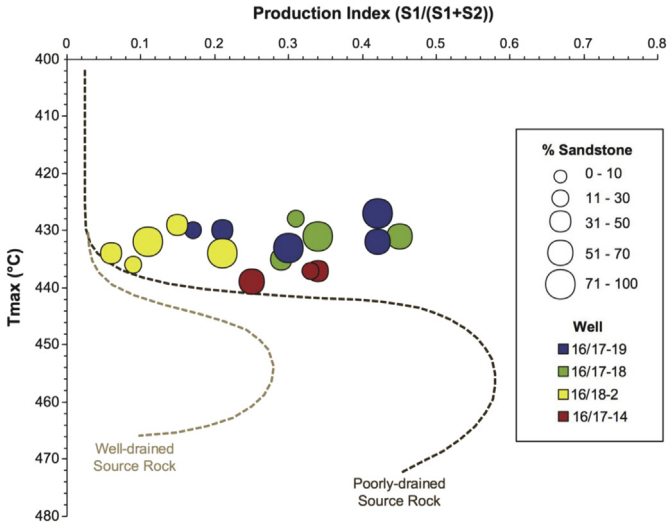

Figure 15. Rock-Eval Production Index (PI) *versus* T_{max} plot with interpretation based on organic rich mudstones.

suggesting low retention of generated oil. Where sandstones dominate (>70% sand), the average PI values are intermediate (0.29–0.31). The changes seen for PI for these essentially iso-maturity samples (Fig. 14) are broken down into the influence of Rock-Eval S2 and S1 (Fig. 16 lower left and right respectively). From these plots it seems that the increase in PI is more to do with a systematic decrease in S2 (generation from kerogen) than an increase in S1 (retention of generated oil). The stratigraphically equivalent public database from adjacent UK and Norwegian wells (shown as red + symbols) confirms that these trends also derive from routine cuttings samples from numerous exploration wells (Fig. 16). It can be concluded that the sand-rich samples have closely grouped low S2 values but more scattered, higher S1 values (Fig. 16) in contrast to the interbedded mudstone-rich samples.

The anomalous individual PI value of 0.42 is observed at 4193.6 m in well 16/17-14, and suggests either the migration of oil into the pore spaces of the sandstones (oil staining), or because the sandstone has reduced kerogen (1.1 wt % TOC). Migration of oil from the mudstone into the interbedded sandstone involves a short vertical distance from the source to storage in the interbeds (Turner et al., 1987; Reitsema, 1983; Roberts, 1991), hence it is concluded that free oil (S1) has migrated into the sand horizons of these finely layered sedimentary facies.

3.5. *Effect of sand content on free oil in sediments*

Rock-Eval S1 is used to measure the quantity of free oil in mg 'oil'/g of source rock in the sampled cores. Plotted against sample depth, and in the context of the local Viking Group mudstones, the core plug Rock-Eval data (Table 1) confirm a deeper zone of high S1 values (Fig. 17, left). Plotted against lithology, the sandstone-dominated samples have lower S1 (free oil) values (1–3 kg/t) than the mudstone-rich samples with S1 values of 3–6 kg/t (Fig. 17, right). A consistent, but poor correlation is observed independent of the well from which the samples were taken. The negative correlation (high S1 = low % sand) suggests that the sandstone

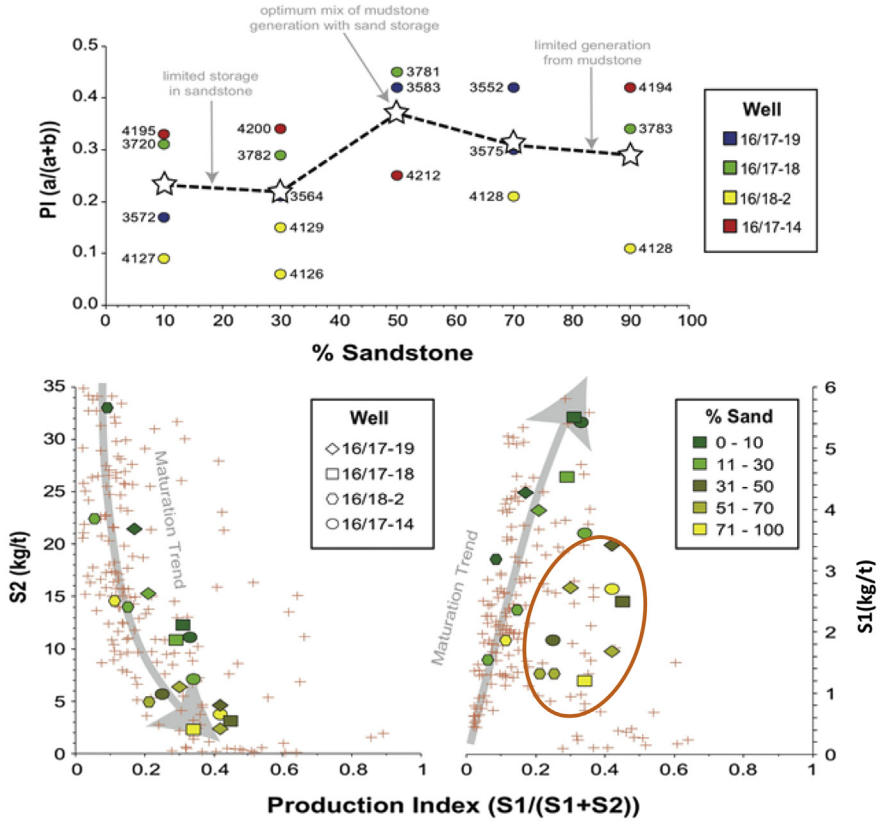

Figure 16. Relationship between sandstone content and Production Index (Upper) and the breakdown of Production Index into contributions from S2 (lower left) and S1 (lower right) yields. For the latter circled cluster = higher PI values for sands with lower S1 yields. Red crosses represent data from the Norwegian Petroleum Directorate (NPD) and other UK North Sea sites. (For interpretation of the references to colour in this figure legend, the reader is referred to the web version of this article.)

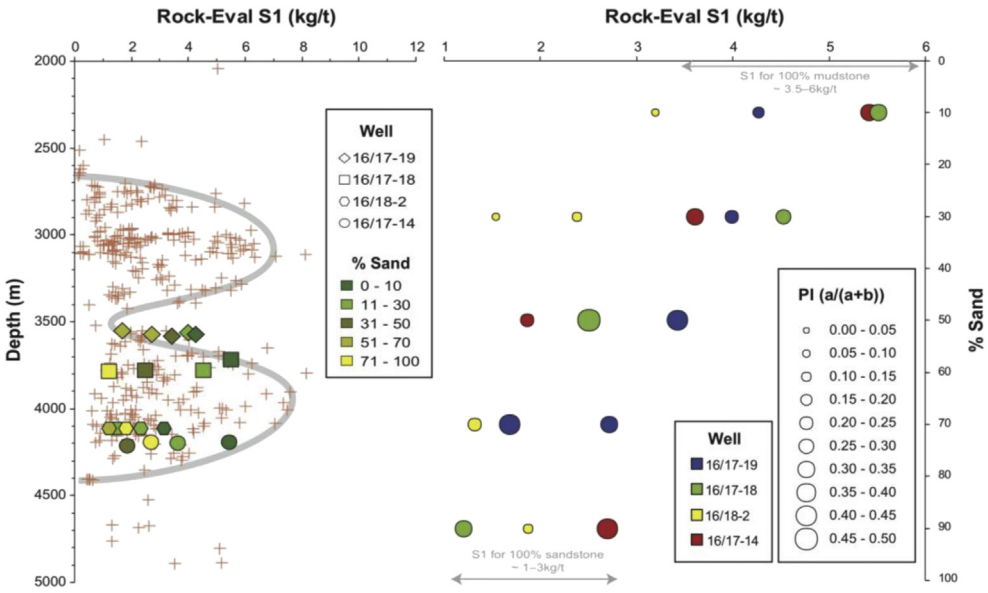

Figure 17. Correlation between % sandstone and S1 (free oil). Red crosses represent data from the Norwegian Petroleum Directorate (NPD) and other UK North Sea sites. (For interpretation of the references to colour in this figure legend, the reader is referred to the web version of this article.)

lithofacies has a lower affinity to absorb the expelled free oil (S1), while the organic-rich mudstone has a higher adsorptive affinity for S1 oil (Fig. 17). In the sample intervals the mudstone S1 values may be considered as 'in situ' free oil, and the sandstone S1 values may be considered as 'migrated', where the migration distance is typically between 0.01 and 10 mm (Figs. 3 and 4).

Jarvie's (2012) plot of S1 *versus* TOC (Fig. 18) discriminates between unconventional productive and unproductive S1 values, and suggests that it is not the absolute value of S1 but the amount of S1 relative to TOC that controls unconventional oil productivity. For the UK Quadrant 16 samples, the Jarvie plot places the sand-rich samples on the productive side of the diagonal boundary, with none of the samples falling clearly within the 'oil shows' region of the plot. The low % sand samples plot in the 'low oil production' area (Fig. 18) though they actually contain higher S1 values than the

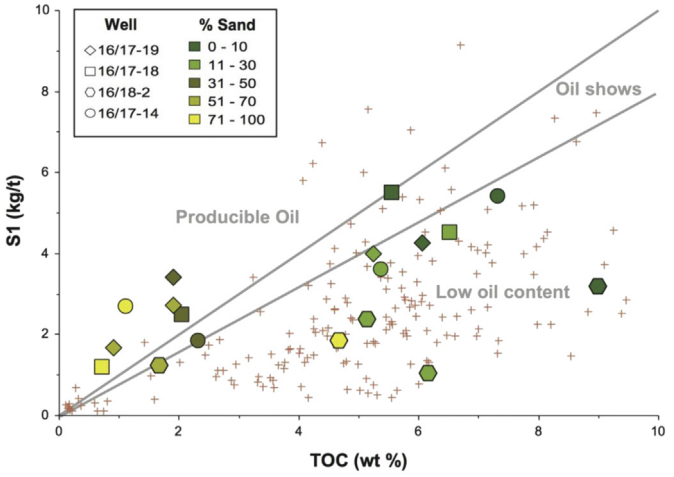

Figure 18. TOC (wt %) *versus* S1 (kg/tonne) plot (after Jarvie, 2012) showing the producible oil content in UK Quadrant 16 samples from this study. Red crosses represent data from the Norwegian Petroleum Directorate Quadrant 15 and UK Quadrant 16 over a similar depth range, 3.5 to 4.5 km. (For interpretation of the references to colour in this figure legend, the reader is referred to the web version of this article.)

sand-dominated samples (Fig. 17 right). Other than the obvious greater storage capacity of the sandstones, this may be due to a number of causes: evaporative losses during core storage or sample preparation, contamination into the sands from drilling fluid, the lack of adsorption of sandstones or the type of oil (lighter oils or volatile). Adsorption affinity is an important factor in hydrocarbon storage, as organic-rich shales tend to hold onto hydrocarbon better than either organic lean rocks (Jarvie, 2014) or rocks predominantly with quartz and carbonate minerals (Schettler and Parmely, 1991). Another technical factor to be considered is that the Rock-Eval 6 instrument has been shown to yield lower S1 values compared to other Rock-Eval instruments (Jarvie, 2014) and therefore, samples with S1/TOC <1 may still be productive. The shale samples co-plotted with a larger background data set of cuttings (symbol = +) from the UK Quadrant 16 and Norwegian Quadrant 15 over a similar depth range (Viking Group samples from 3.5 to 4.5 km).

This interpretation suggests that the optimal unconventional samples have >50% sand and TOC values in the 1–2% range (Fig. 16 upper and Fig. 18). The ratio of S1/TOC forms the Oil Saturation Index (OSI = S1 kg/tonne/(wt % TOC/100) as defined by Jarvie (2012), which shows higher OSI values for sandstone-rich samples relative to mudstone samples (Fig. 19). Jarvie (2012) proposes that values greater than 100 (e.g., TOC = 3%, S1 = 3 kg/t) are prospective for shale oil exploitation, which again is confined to samples with >50% sandstone for the UK Quadrant 16 sample set.

At an early stage of maturation, the oil generated from kerogen in the mudstones will start to saturate any available porosity. With increasing maturation, the mudstone porosity will be filled and, subject to adequate permeability, localised expulsion will start to fill the open pore spaces of sandstones in close proximity. The mudstones will contain the retained oil prior to, during and after expulsion. This also emphasises that the new S1 data broadly fit the distribution from cuttings samples of Viking Group shales taken from numerous wells in adjacent areas.

This simple calculation shows that, given the typical densities ($\rho_{rock} = 2.65$ g/cm^3; $\rho_{kerogen} = 1.40$ g/cm^3; $\rho_{oil} = 0.86$ g/cm^3), 6 wt % TOC occupies about 11 volume % of the sediment, and that the S1 value of 5 kg/tonne (typical for pure Kimmeridge Clay shales at this

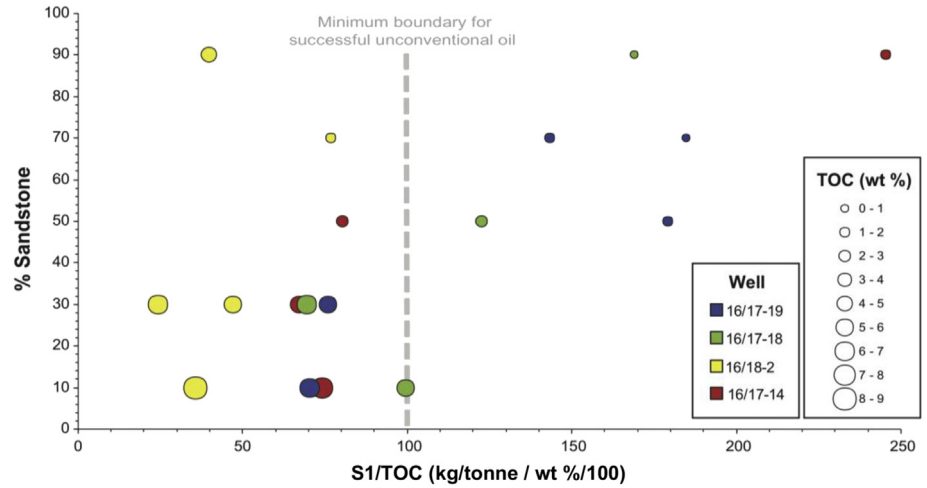

Figure 19. Relationship between the Oil Saturation Index *versus* estimated % sandstone showing samples predicted to contain producible oil when OSI is greater than 100. This boundary restricts unconventional oil productivity to the more sand-prone and lower TOC samples.

maturity level – see Fig. 14) occupies about 1.54 volume % of the rock. Measuring the porosities of fine grained rocks is problematic depending on the method of determination, grain size, mineralogy and burial depth (Swarbrick and Osborne, 1998). Based on lab measurements of helium porosity and QEM scanning electron microscopy of Kimmeridge Clay mudstone core plugs from UK Quadrant 16, Cornford et al. (2014), reported mean porosity values of 2.58 ± 1.14% (n = 15) and 1.62 ± 1.41% (n = 34), respectively, for the two methods. Taking an average of 2% volume 'available' porosity (where 'available' excludes residual water saturation and closed porosity), and S1 values of 1.5% volume, the 'oil' saturation of the porosity of the sampled mudstone is about 75%. Gas and light hydrocarbon loss from S1 during sampling and sample preparation may make this value up to 100% as expected for samples taken in the oil expulsion window. This analysis indicates that for pure mudstone, full saturation of the 'available' porosity limits the retained oil available for unconventional exploitation.

The expulsion process results in some changes in the chemical composition through geo-chromatography fractionation leading to the expulsion of less polars and asphaltenes and more saturates in the expelled oil (Leythaeuser et al., 1984), leaving the retained 'residual' oil conversely enriched. Geo-chromatographic fractionation of the expelled oil would likely occur as the oil undergoes expulsion and migration from the source rock into non-source rocks. In this process, the heavy oil with more polar hydrocarbon components is retained in the mudstones (potentially adsorbed on to clay mineral surfaces), while the lighter oil is drained into the interbedded sandstones.

These organic-lean, but oil mature interbedded sandstones would be expected to have free oil (S1) stored in their pores resulting in high productivities due to the short distances required for the migration of weakly adsorbed oil within the porous intervals (Leythaeuser et al., 1982, 1984, 1987). The lower S1 values in the sandstone-rich samples (Figs. 16 and 19) may derive from a number of processes:

1. The oil failed to move from the shales into the sands, possibly due to overpressure developed in isolated sand lenses reducing the pressure potential gradient
2. During drilling of the cores, oil was more effectively flushed from the sand compared to the mudstone interbeds
3. Migration into sandstone may also have occurred because these wells were drilled 'on structure' and hence are plumbed into the main migration path (drained sand). As such, the oil may have locally migrated into the sandstones from the mudstones a few cm away, or migrated from deeper in the basin, and then up dip to the basin margin structures.

All of these three factors will arguably have had some influence on the oil saturation of the sand layers. With reference to Figures 16 and 20, if the initial S2 potential of 27 kg/ton is eventually converted to oil (S1) and only 5 kg/ton is retained, then 22 kg/ton (2.2 wt%) or 6.82% volume oil will be lost from fully mature mudstones. Taking a cubic metre of oil mature 50% mudstone/50% sandstone, and given the observed porosity range of 5–10% for Brae Formation sandstones at 4 km (Cornford et al., 2014), the expelled oil volume of 6.8% equates approximately to a mid-range porosity for an equal volume of sandstone (Fig. 20).

4. Conclusions

Integration of geochemical and mineralogy data from oil-mature core samples from wells in the UK North Sea Quadrant 16 demonstrate some of the effects of sand interbeds on the likely unconventional shale reservoir properties. North Sea Kimmeridge Clay Formation with interbedded mudstones and sandstones contains significant amount of expelled oil in the sands, as well as retained oil in the muds. Distal and inter-fan areas allow development of a hybrid system (frack production from both mudstones

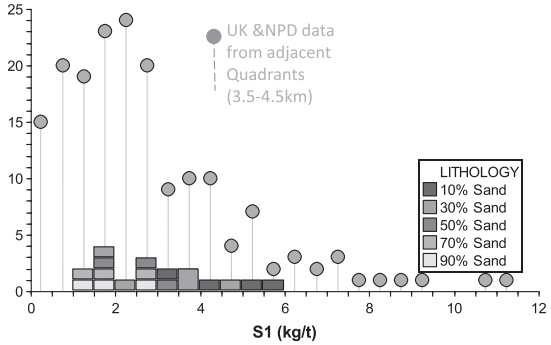

Figure 20. Distribution of S1 (free oil) values for the project core plug samples and Viking Group cuttings from adjacent UK and Norwegian wells in the 3.5–4.5 km range.

and sandstones), and selection of optimum sand-shale ratio for unconventional oil exploitation.

The abundance and preservation of silicate minerals in the sand-rich samples suggest little diagenetic alteration which is likely to exert control on the brittleness of the interbedded sandstone and mudstone. Finding an area in this hybrid system that is brittle may be a key factor in creating vertical fracture pattern that are extensive enough to connect and drain the optimum rock volume during hydraulic fracturing stimulation.

The amount of kerogen, as measured by TOC, is higher in the mudstone-dominated samples (6.3 wt % average) than in the sandstone dominated samples (1.4 wt % average), with projected pure end members being 9 wt% and 0.5 wt % respectively. A dilution model is confirmed by the uniformity of the bulk kerogen type as measured by Rock-Eval Hydrogen Indices, based on HI-T_{max} trends and confirmed by a larger data set of cuttings analyses from adjacent Norwegian wells. The kerogen type in both the mudstones and sandstones is predominantly a classical Type II oil (and associated gas) prone kerogen. The mudstone-dominated samples, with low sedimentation rates, show mildly increasing (heavier) isotope values per 1% increase in TOC, which would be consistent with a dominance of sulphate-reducing bacterial degradation. In contrast, the sandstone-dominated samples, with higher sedimentation rates, show strongly increasing (heavier) kerogen isotope values per 1% increase in TOC, suggesting degradation dominated by methanogenesis. Rock-Eval T_{max} values of 432 °C (early mature) to 439 °C (mid-mature) equate to the 3–4 km interval placing the samples in a limited range of early oil window maturation for the sampled mudstones and sandstone interbeds. Based on US analogues, this maturity level is lower than claimed as optimum for extraction of 'volatile oil' by hydraulic fracking.

Migration of free oil (S1) from the mudstone into the interbedded sandstone involves a short lateral distance through the sandstone pores from the source to storage in the interbeds resulting in high productivities. Therefore, the conclusion is that free oil (S1) has migrated into the sandy layers, implying that the sand-rich samples have retained rather than drained oil. The abundance of sandy layers would be expected to define drainage. However, the relationship between PI and T_{max} suggest these bulk samples to be poorly-drained source rocks at the maturity levels encountered.

The Oil Saturation Index (OSI = S1/TOC) shows higher values for sandstone-rich samples relative to the mudstones, and higher values for lower TOC samples at the encountered early-mature level of maturation. These data suggest that the optimal unconventional samples have ~50% sand and TOC values in the range of 1–2%. The key points of this hybrid system are the thickness, storage capacity and the possibility to capture a portion of the expelled as well as retained oil.

Acknowledgements

The authors would like to thank Trapoil and Two Fields Consulting (TFC) for supporting this research. HCG thanks the Royal Society for an Industry Fellowship. MR acknowledges receipt of a Durham University Doctoral Scholarship (DDS). Funding for the new geochemical work in this paper was partially funded by a Natural Environment Research Council grant to Darren Gröcke (NE/H021868/1). We are grateful to the British Geological Survey (BGS) for providing the core samples for this study, and Applied Petroleum Technology (APT) for rapid analyses of these samples. A special thanks goes to Integrated Geochemical Interpretation Limited (IGI Ltd) for the use of their p: IGI-3 software for the geochemical interpretation of the results. The authors wish to acknowledge important contributions and review by Dan Jarvie, and an anonymous reviewer.

References

Abrams, M.A., Dieckmann, V., Curiale, J.A., Clark, R., 2014. Hydrocarbon Charge Considerations in Liquid-rich Unconventional Petroleum Systems. American Association of Petroleum Geologists Search and Discovery Article, #80366.

Arduini, M., Golfetto, F., Ortenzi, A., 2009. The Chlorite-bearing Reservoirs: Effects of the Main Petrographic Parameters on Reservoir Quality. American Association of Petroleum Geologists Search and Discovery Article #50178.

Baird, R.A., 1986. Maturation and source rock-evaluation of Kimmeridge Clay, Norwegian North Sea. Am. Assoc. Pet. Geol. Bull. 70, 1–11.

Barnard, P.C., Cooper, B.S., 1981. Oils and source rocks of the North Sea area. In: Illing, L.V., Hobson, G.D. (Eds.), Petroleum Geology of the Continental Shelf of Northwest Europe. Heyden, London, Institute of Petroleum, pp. 169–175.

Bernard, P.C., Collins, A.G., Cooper, B.S., 1981. Identification and distribution of kerogen facies in a source rock horizon—examples from the North Sea basin. In: Brooks, J. (Ed.), Organic Maturation Studies and Fossil Fuel Exploration. Academic Press, London, pp. 271–282.

Bernard, S., Brown, L., Wirth, R., Schreiber, A., Schulz, H.-M., Horsfield, B., Aplin, A.C., Mathia, E.J., 2013. FIB-SEM and TEM investigations of an Organic-rich Shale Maturation Series from the Lower Toarcian Posidonia Shale, Germany: Nanoscale pore system and fluid-rock interactions. AAPG Mem. Electron Microsc. Shale Hydrocarb. Reserv. 102, 53–66.

Calvert, S.E., 2004. Beware intercepts: interpreting compositional ratios in multicomponent sediments and sedimentary rocks. Org. Geochem. 35, 981–987.

Chalmers, G.R.L., Bustin, R.M., 2012. Geological evaluation of Halfway-Doig-Montney hybrid gas shale-tight gas reservoir, northeastern British Columbia. Mar. Pet. Geol. 38, 53–72.

Chalmers, G.R.L., Bustin, R.M., Bustin, A.A.M., 2012. Geological Controls on Matrix Permeability of the Doig-Montney Hybrid Shale-gas-tight-gas Reservoir, Northeastern British Columbia (NTS 093P). In Geoscience BC Summary of Activities 2011, Geoscience BC, Report 2012-1, pp. 87–96.

Cooper, B.S., Barnard, P.C., 1984. Source rocks and oils of the central and northern North Sea. In: Demaison, G., Murris, R.J. (Eds.), Petroleum Geochemistry and Basin Evaluation, American Association of Petroleum Geologists Memoir 35, pp. 303–314.

Cooper, B.S., Bernard, P.C., Telnaes, N., 1995. The Kimmeridge Clay formation of the North Sea. In: Katz, B.J. (Ed.), Petroleum Source Rocks. Springer-Verlag, Berlin, pp. 89–110.

Cornford, C., 1984. Source rocks and hydrocarbons of the North Sea. In: Glennie, K.W. (Ed.), Introduction to the Petroleum Geology of the North Sea. Blackwell Scientific Publications, Oxford, pp. 171–209.

Cornford, C., 1998. Source rocks and hydrocarbons of the North Sea. In: Glennie, K.W. (Ed.), Petroleum Geology of the North Sea (4th eds). Blackwell Science Ltd., London, pp. 376–462.

Cornford, C., Brooks, J., 1989. Tectonic controls on oil and gas occurrences in the North Sea area. In: Tankard, A.J., Balkwill, H.R. (Eds.), Extensional Tectonics and Stratigraphy of the North Atlantic Margins. American Association of Petroleum Geologists/Canadian, Geological Foundation, 46–641.

Cornford, C., Morrow, J.A., Turrington, A., Miles, J.A., Brooks, J., 1983. Some geological controls on oil composition in the UK. North Sea. In: Brooks, J. (Ed.), Petroleum Geochemistry and Exploration of Europe, Geological Society Special Publication, Blackwell Scientific Publications, Oxford, 12, pp. 175–194.

Cornford, C., Birdsong, B., Groves, G., 2014. Offshore unconventional oil from the Kimmeridge Clay Formation of the North Sea: a technical and economic case. In: Unconventional Resources Technology Conference Proceedings, August 25–27, 2014.

Department of Energy and Climate Change (DECC), 2013. United Kingdom Continental Shelf (UKCS) Geological Basins. Available online: https://www.gov.uk/oil-and-gas-offshore-maps-and-gis-shapefiles20140331_UKCS_Geological_Basin (accessed 12.03.14.).

Dominguez, R., 2007. Structural evolution of the Penguins Cluster, UK Northern North Sea. Geol. Soc. Lond. Spec. Publ. 292, 25–48. http://dx.doi.org/10.1144/SP292.2.

Erratt, D., Thomas, G.M., Hartley, N.R., Musum, R., Nicholson, P.H., Spisto, Y., 2010. North Sea hydrocarbon systems: some aspects of our evolving insights into a classic hydrocarbon province. In: Vining, B., Pickering, S.C. (Eds.), Petroleum Geology: from Mature Basins to New Frontiers—Proceedings of the 7th Petroleum Geology Conference. Geological Society of London, London, England, pp. 37–56.

Espitalié, J., Deroo, G., Marquis, F., 1985. La pyrolyse Rock-Eval etses applications. Première Partie. Rev. Inst. Fr. Pét. 40, 563–579.

Faerseth, R.B., 1996. Interaction of Permo-Triassic and Jurassic extensional fault blocks during the development of the northern North Sea. J. Geol. Soc. Lond. 153, 931–944. http://dx.doi.org/10.1144/gsjgs.153.6.0931.

Farrimond, P., Comet, P., Eglinton, G., Evershed, R.P., Hall, M.A., Park, D.W., Wardroper, A.M.K., 1984. Organic geochemical study of the Upper Kimmeridge Clay of the Dorset type area. Mar. Pet. Geol. 1, 340–354.

Fuller, J.G.C.M., 1980. Progress report on fossil fuels—exploration and exploitation. In: Jones, J.M., Scott, P.W. (Eds.), Proceedings of Yorkshire Geology Society, vol. 33, pp. 581–593.

Galimov, E.M., 2006. Isotope organic geochemistry. J. Org. Geochem. 37 (10), 1200–1262.
Gautier, D.L., 2005. Kimmeridgean Shales Total Petroleum System of the North Sea Graben Province: U.S. Geological Survey Bulletin 2204-C, 24. Available online: http://pubs.usgs.gov/bul/2204/c (accessed 15.06.14.).
Glennie, K.W., 1986. Development of northwest Europe's southern Permian gas basin. In: Brooks, J., Goff, J.C., van Hoorn, B. (Eds.), Habitat of Palaeozoic Gas in NW Europe, Geological Society, London, Special Publication 23, pp. 3–22.
Gluyas, J., Garland, C., Oxtoby, N.H., Hogg, A.J.C., 2000. Quartz cement: the Miller's tale. In: Worden, R.H., Morad, S. (Eds.), Quartz Cementation in Sandstones, International Association of Sedimentology Special Publication 29, pp. 199–218.
Goff, J.C., 1983. Hydrocarbon generation and migration from Jurassic source rocks in the East Shetland Basin and Viking Graben of the northern North Sea. J. Geol. Soc. 140, 445–474.
Gröcke, D.R., Ludvigson, G.A., Witzke, B.L., Robinson, S.A., Joeckel, R.M., Ufnar, D.F., Ravn, R.L., 2006. Recognizing the Albian-Cenomanian (OAE1d) sequence boundary using plant carbon isotopes: Dakota Formation, Western Interior Basin, USA. Geology 34, 193–196.
Hallam, A., Grose, J.A., Ruffell, A.H., 1991. Palaeoclimatic significance of changes in clay mineralogy across the Jurassic–Cretaceous boundary in England and France. Palaeogeogr. Palaeoclimatol. Palaeoecol. 81, 173–187.
Hesselbo, S., Deconinck, J.-F., Huggett, J.M., Helen, S., 2009. Late Jurassic Palaeoclimatic change from clay mineralogy and gamma-ray spectrometry of the Kimmeridge Clay, Dorset, UK. J. Geol. Soc. 166, 1123–1133.
Hillier, S., Matyas, J., Matter, A., Vasseur, G., 1995. Illite/smectite diagenesis and its variable correlation with vitrinite reflectance in the Pannonian Basin. Clays Clay Minerals 43 (2), 174–183.
Huc, A.Y., Irwin, H., Schoell, M., 1985. Organic matter quality changes in an Upper Jurassic shale sequence from the Viking Graben. In: Thomas, B.M., Doré, A.G., Eggen, S.S., Home, P.C., Larsen, R.M. (Eds.), Petroleum Geochemistry in Exploration of the Norwegian Shelf. Graham and Trotman, London, pp. 179–183.
Isaksen, G.H., Ledje, K.H.I., 2001. Source rock quality and hydrocarbon migration pathways within the greater Utsira High area, Viking Graben, Norwegian North Sea. Am. Assoc. Pet. Geol. Bull. 85 (5), 861–883.
Isaksen, G.H., Patience, R., van Graas, G., Jenssen, A.I., 2002. Hydrocarbon system analysis in a rift basin with mixed marine and non-marine source rocks; the South Viking Graben, North Sea. Am. Assoc. Pet. Geol. Bull. 86 (4), 557–591.
Jarvie, D.M., 2012. Shale resource systems for oil and gas: part 1 shale-gas resource systems. In: Breyer, J.A. (Ed.), Shale Reservoirs Giant Resources for the 21st Century, American Association of Petroleum Geologists Memoir 97, pp. 69–87.
Jarvie, D.M., 2014. Components and processes affecting producibility and commerciality of shale resource systems. ALAGO 2012 Special Publication GeologicaActa 12 (4), 307–325.
Jarvie, D.M., Brenda, L.C., Floyd "Bo", H., Breyer, John T., 2001. Oil and Shale Gas from the Barnett Shale, Ft. Worth Basin, Texas. AAPG National Convention, June 3–6, 2001, Denver, CO. In: American Association of Petroleum Geologists Bulletin 85, 13 (Supplement), A100.
Jarvie, D.M., Hill, R.J., Ruble, T.E., Pollastro, R.M., 2007. Unconventional shale gas systems: the Mississippian Barnett Shale of north-central Texas as one model for thermogenic shale gas assessment. Am. Assoc. Pet. Geol. Bull. 91, 475–499.
Jarvis, I., Lignum, J.S., Gröcke, D.R., Jenkyns, H.C., Pearce, M.A., 2011. Black shale deposition, atmospheric CO_2 drawdown, and cooling during the Cenomanian–Turonian Oceanic Anoxic Event. Paleoceanography 26 (3). PA3201.
Jenkyns, H.C., Jones, C.E., Gröcke, D.R., Hesselbo, S.P., Parkinson, D.N., 2002. Chemostratigraphy of the Jurassic System: applications, limitations and implications for palaeoceanography. J. Geol. Soc. London 159, 351–378.
Johnson, H., Leslie, A.B., Wilson, C.K., Andrews, I.J., Cooper, R.M., 2005. Middle Jurassic, Upper Jurassic and Lower Cretaceous of the UK Central and Northern North Sea, p. 42. British, Geological Survey Research Report, RR/03/001.
Junium, C.K., Arthur, M.A., 2007. Nitrogen cycling during the Cretaceous, Cenomanian-Turonian Oceanic Anoxic Event II. Geochem. Geophys. Geosyst. 8, 3. http://dx.doi.org/10.1029/2006GC001328.
Justwan, H., Dahl, B., Isaksen, G.H., Meisingset, I., 2005. Late to Middle Jurassic source facies and quality variations, South Viking Graben, North Sea. J. Pet. Geol. 28 (3), 241–268.
Justwan, H., Dahl, B., Isaksen, G.H., 2006. Geochemical characterization and genetic origin of oils and condensates in the South Viking Graben, Norway. J. Mar. Pet. Geol. 23, 213–239.
Kemp, S.J., Bouch, J., Murphy, H.M., 2001. Mineralogical Characterisation of the Nordland Shale, UK Quadrant 16, Northern North Sea. British Geological Survey Commissioned Report, CR/01/136, 52.
Kwon, O., Herber, B.E., Kronenberg, A.K., 2004. Permeability of illite-bearing shale: 2. Influence of fluid chemistry on flow ad functionally connected pores. J. Geophys. Res. B10206. http://dx.doi.org/10.1029/2004B003055.
Lafargue, E., Marquis, F., Pillot, D., 1998. Rock-Eval 6 applications in hydrocarbon exploration, production, and soil contamination studies. Rev. Inst. Fr. Pét. 53, 421–437.
Leythaeuser, D.R., Schaefer, G., Yukler, A., 1982. Role of diffusion in primary migration of hydrocarbons. Am. Assoc. Pet. Geol. Bull. 66 (4), 408–429.
Leythaeuser, D., Radke, M., Schaefer, R.G., 1984. Efficiency of petroleum expulsion from shale source rocks. Nature 311, 745–748.
Leythaeuser, D., Schaefer, R.G., Radke, M., 1987. On the primary migration of petroleum. In: Special Paper Proceedings of the 12th World Petroleum Congress. John Wiley & Sons Limited, Chichester, pp. 227–236.
Lothe, A.E., Zweigel, P., 1999. Saline Aquifer CO_2 Storage (SACS). In: Informal Annual Report 1999 of SINTEF Petroleum Research's Results in Work Area 1 'Reservoir Geology'. SINTEF Petroleum Research report 23.4300.00/03/99, 54.
Loucks, R.G., Reed, R.M., Ruppel, S.C., Jarvie, D.M., 2009. Morphology, Genesis, and distribution of Nanometer-Scale pores in siliceous mudstones of the Mississippian Barnett Shale. J. Sediment. Res. 79, 848–861.
Marchand, A.M.E., Craig Smalley, P.C., Haszeldine, R.S., Fallick, A.E., 2002. Note on the importance of hydrocarbon fill for reservoir quality prediction in sandstones. Am. Assoc. Pet. Geol. Bull. 86 (9), 1561–1571.
Meyers, P.A., 1994. Preservation of source identification of sedimentary organic matter during and after deposition. Chem. Geol. 144, 289–302.
Meyers, P.A., Benson, L.V., 1988. Sedimentary biomarker and isotopic indicators of the paleoclimatic history of the Walker Lake basin, western Nevada. Org. Geochem. 13, 807–813.
Meyers, P.A., Eadie, B.J., 1993. Sources, degradation and recycling of organic matter associated with sinking particles in Lake Michigan. Org. Geochem. 20, 47–56.
Meyers, P.A., Leenheer, M.J., Eadie, B.J., Maule, S.J., 1984. Organic geochemistry of suspended and settling particulate matter in Lake Michigan. Geochim. Cosmochim. Acta 48, 443–452.
Moore, D.M., Reynolds Jr., R.C., 1997. X-Ray Diffraction and the Identification and Analysis of Clay Minerals, second ed. Oxford University Press, New York.
NIGOGA: The Norwegian Guide to Organic Geochemical Analyses. http://www.npd.no/engelsk/nigoga/default.htm (accessed 10.05.14.).
Norwegian Petroleum Directorate (NPD). Available online: http://www.npd.no/en/ (accessed 18.04.14.).
Partington, M.A., Mitchener, B.C., Milton, N.J., Fraser, A.J., 1993. Genetic sequence stratigraphy for the North Sea Late Jurassic and early Cretaceous: distribution and prediction of Kimmeridgian-Late Ryazanian reservoirs in the North Sea and adjacent areas. In: Parker, J.R. (Ed.), Petroleum Geology of Northwest Europe: Proceedings of the 4th Conference on Petroleum Geology of NW. Europe, at the Barbican Centre, London. Geological Society, London, pp. 347–370.
Pearson, M.J., Watkins, D., Pittion, J.-L., Caston, D., Small, J.S., 1983. Aspects of burial diagenesis, organic maturation and palaeothermal history of an area in the South Viking Graben, North Sea. In: Brooks, J. (Ed.), Petroleum Geochemistry and the Exploration of Europe. Blackwell, Oxford, pp. 161–173.
Peters, K.E., 1986. Guidelines for evaluating petroleum source rock using programmed pyrolysis. Am. Assoc. Pet. Geol. Bull. 70, 329.
Peters, K.E., Walters, C.C., Moldowan, J.M., 2005. The Biomarker Guide, second ed. Cambridge University Press, Cambridge, UK.
Reitsema, R.H., 1983. Geochemistry of North and South Brae areas, North Sea. In: Brooks, J. (Ed.), Petroleum Geochemistry and Exploration of Europe, Geological Society, London, Special Publication, 12, pp. 203–212.
Richards, P.C., Lott, G.K., Johnson, H., Knox, R.W.O.'B., Riding, J.B., 1993. Jurassic of the Central and Northern North Sea. In: Knox, R.W.O.'B., Cordey, W.G. (Eds.), Lithostratigraphy Nomenclature of the UK North Sea. British Geological Survey, Nottingham, 1–252.
Roberts, M.J., 1991. The South Brae Field, Block 16/7a, U.K. North Sea. In: Abbotts, I.L. (Ed.), United Kingdom Oil and Gas Fields 25 Years Commemorative Volume, Geological Society, London, Memoir, 14, pp. 55–62.
Rooksby, S.K., 1991. The Miller Field, Blocks 16/7B, 16/8B, UK North Sea. Geol. Soc. Lond. Mem. 4, 159–164.
Schaefer, R.G., Schenk, H.J., Harms, R., 1990. Determination of gross kinetic parameters for petroleum formation from Jurassic source rocks of different maturity levels by means of laboratory experiments. Adv. Org. Geochem. 16 (I-3), 115–120.
Schettler Jr., P.D., Parmely, C.R., 1991. Contributions to total storage capacity in Devonian shales. Soc. Pet. Eng. 23422, 9.
Schlakker, A., Csizmeg, J., Pogácsás, G., Horti, A., 2012. Burial, Thermal and Maturation History in the Northern Viking Graben (North Sea).American Association of Petroleum Geologists Search and Discovery Article #50545. Poster Presentation at AAPG International Convention and Exhibition, Milan, Italy. October 23–26, 2011.
Spence, S., Kreutz, H., 2003. The Kingfisher Field, Block 16/8a, UK North Sea. Geol. Soc. Lond. Mem. 20, 305–314.
Stow, D.A.V., 1983. Sedimentology of the Brae oilfield, North Sea: a reply. J. Pet. Geol. 6, 103–104.
Swarbrick, R.E., Osborne, M.J., 1998. Mechanisms that generate abnormal pressures: an overview. In: Law, B.E., Ulmishek, G.F., Slavin, V.I. (Eds.), Abnormal Pressures in Hydrocarbon Environments, American Association of Petroleum Geologist Memoir 70, pp. 13–34.
Turner, C.C., Cohen, J.M., Connel, J.R., Cooper, D.M., 1987. A depositional model for the South Brae oilfield. In: Brooks, J., Glennie, K.W. (Eds.), Petroleum Geology of North West Europe, London. Graham and Trotman, pp. 853–864.
Tyson, R.V., 2004. Variation in marine total organic carbon through the type Kimmeridge Clay Formation (Late Jurassic), Dorset, UK. J. Geol. Soc. 161, 667–673.
Underhill, J.R., 1998. Jurassic. In: Glennie, K. (Ed.), Introduction to the Petroleum Geology of the North Sea. Blackwell Science, pp. 245–293.
Weiss, H.M., Wilhelms, A., Mills, N., Scotchmer, J., Hall, P.B., Lind, K., Brekke, T., 2000. NIGOGA – the Norwegian Industry Guide to Organic Geochemical Analyses [online]. Edition 4.0 Published by Norsk Hydro, Statoil, GeolabNor, SINTEF Petroleum Research and the Norwegian Petroleum Directorate, 102. Available online: http://www.npd.no/engelsk/nigoga/default.htm (accessed 10.05.14.).
Ziegler, P.A., 1990. Tectonic and palaeogeographic development of the North Sea rift system. In: Blundell, D.J., Gibbs, A.D. (Eds.), Tectonic Evolution of the North Sea Rifts. Oxford University Press, New York, pp. 1–36.